Insect Systematics and Diversity, (2021) 5(5): 7; 1–18
https://doi.org/10.1093/isd/ixab018
Invited Article

ENTOMOLOGICAL SOCIETY OF AMERICA
SHARING INSECT SCIENCE GLOBALLY

OXFORD

Molecular phylogenetics, phylogenomics, and phylogeography

Is Phylogeographic Congruence Predicted by Historical Habitat Stability, or Ecological Co-associations?

Ryan C. Garrick,[1,5] Chaz Hyseni,[1,2] Ísis C. Arantes,[1] Louis G. Zachos,[3] Peter C. Zee,[1] and Jeffrey C. Oliver[4]

[1]Department of Biology, University of Mississippi, Oxford, MS 38677, USA, [2]Department of Ecology and Genetics, Uppsala University, Norbyvägen 18 D, 75236, Uppsala, Sweden, [3]Department of Geology and Geological Engineering, University of Mississippi, Oxford, MS 38677, USA, [4]Office of Digital Innovation and Stewardship, University of Arizona, Tucson, AZ 85724, USA, and [5]Corresponding author, e-mail: rgarrick@olemiss.edu

Subject Editor: Jeffrey Lozier

Received 26 February 2021; Editorial decision 12 July 2021

Abstract

Comparative phylogeographic studies can distinguish between idiosyncratic and community-wide responses to past environmental change. However, to date, the impacts of species interactions have been largely overlooked. Here we used non-genetic data to characterize two competing scenarios about expected levels of congruence among five deadwood-associated (saproxylic) invertebrate species (i.e., a wood-feeding cockroach, termite, and beetle; a predatory centipede, and a detritivorous millipede) from the southern Appalachian Mountains—a globally recognized center of endemism. Under one scenario, abiotic factors primarily drove species' responses, with predicted congruence based on the spatial overlap of climatically stable habitat areas estimated for each species via ecological niche modeling. The second scenario considered biotic factors to be most influential, with proxies for species interactions used to predict congruence. Analyses of mitochondrial and nuclear DNA sequences focused on four axes of comparison: the number and geographic distribution of distinct spatial-genetic clusters, phylogeographic structure, changes in effective population size, and historical gene flow dynamics. Overall, we found stronger support for the ecological co-associations scenario, suggesting an important influence of biotic factors in constraining or facilitating species' responses to Pleistocene climatic cycles. However, there was an imperfect fit between predictions and outcomes of genetic data analyses. Thus, while thought-provoking, conclusions remain tentative until additional data on species interactions becomes available. Ultimately, the approaches presented here advance comparative phylogeography by expanding the scope of inferences beyond solely considering abiotic drivers, which we believe is too simplistic. This work also provides conservation-relevant insights into the evolutionary history of a functionally important ecological community.

Key words: Appalachian Mountain, comparative phylogeography, ecological niche modeling, saproxylic invertebrate, species interaction

Phylogeographic studies provide important foundations for understanding evolution within, and divergence among, natural populations. Investigations that incorporate models of long-term population history have shed light upon processes that generate, maintain, or compromise the integrity of species boundaries (Moritz et al. 2009). They have also revealed circumstances where gene pools change in counterintuitive ways, such as when drift predominates in large populations (Excoffier and Ray 2008), or where selection is efficient in small populations (Facon et al. 2011). Phylogeographic studies have immediate practical importance too. For instance, they have generated insights into the complexity of responses to past climate change, showing that species did not simply shift in latitudinal or altitudinal range (Blois et al. 2013), and they have provided critical baselines for predicting future impacts (McLachlan et al. 2005, Cordellier and Pfenninger 2009). Notably, phylogeographic studies that identify processes and events that shaped patterns of spatial-genetic variation in multiple co-distributed species can distinguish between idiosyncratic and community-wide responses (Avise 2000, Arbogast and Kenagy 2001), and as such, provide more broadly generalizable inferences.

Climatic Stability

Comparative phylogeographic studies have identified events that drive co-vicariance, such as seaway incursions (Riddle and Hafner 2006) or xerification of mesic habitats (Carstens et al. 2005). Co-expansion in response to amelioration of Pleistocene glaciation or periglaciation has also been characterized (e.g., Lessa et al. 2003, Chan et al. 2014). However, spatial patterns of intraspecific diversity are not simply overwritten by each successive event; long-term climatic stability can itself be a strong predictor of phylogeographic structure, particularly in low-mobility taxa. For example, in the Australian Wet Tropics, climatic stability closely predicted the number and/or distribution of distinct lineages within a suite of rainforest fauna (Hugall et al. 2002) and it also had good explanatory power for spatial patterns of species richness (Graham et al. 2006). Similarly, for reptiles and amphibians in the Brazilian Atlantic forest, historically stable areas often contain high intraspecific genetic diversity and phylogeographic endemism (Carnaval et al. 2009, 2014). However, climatic stability is not a panacea for predicting locations of shared refugia, and by extension, congruence among co-distributed species. A likely explanation for this lies in the heavy reliance of ecological niche models (ENMs, often used to identify long-term stable areas) on just a few abiotic variables, such as temperature and precipitation (Godsoe and Harmon 2012). Accordingly, the incorporation of biotic components that might also have impacted species' responses to past environmental change is imperative.

Ecological Co-associations

Species undoubtedly have evolutionary histories shaped by biotic influences, and the ramifications of ignoring impacts of species interactions on the phylogeographic structure may be considerable. Indeed, sympatry of two or more lineages may be prevented by deterministic processes such as competitive exclusion, or alternatively, by stochastic processes such as priority effects (Crespi et al. 2003, Waters 2011). The results of this ecological exclusion can extend across large spatial and temporal scales (Pigot and Tobias 2013). While taxa with obligate co-associations may be most likely to show lock-step responses to past environmental change (e.g., Smith et al. 2008, 2011; Garrick et al. 2013, 2017), few comparative phylogeographic studies have considered different levels of interdependence among a suite of species (but see Satler and Carstens 2016). Thus, important questions remain unanswered, such as: to what extent do ecological co-associations constrain species' responses to environmental change; at what level of co-association does the biotic constraint become negligible; and what aspect(s) of species interaction matter most?

Southern Appalachian Mountains

Here we investigated whether phylogeographic congruence is predicted by historical habitat stability, or ecological co-associations, using five invertebrate species from the southern Appalachian Mountains, USA. This landscape setting is composed of several physiographic subregions that contain some of the oldest uplands in North America, and it remained unglaciated during the Last Glacial Maximum (~22 thousand years ago, KYA; Whittaker 1956, Delcourt and Delcourt 1998, Loehle 2007). The southern Appalachians served as a source for recolonization of glaciated northern areas after the Laurentide ice sheet retreated (e.g., Herman and Bouzat 2016, Park and Donoghue 2019), and thus harbored important Pleistocene microrefugia. These characteristics enabled in situ persistence of divergent lineages that evolved on the backdrop of steep environmental gradients within a topographically complex region (Hyseni and Garrick 2019a). The resulting impacts upon structuring biodiversity over fine spatial scales, particularly in low-mobility species occupying mid- to high elevations, are conducive to historical inference (Cruzan and Templeton 2000).

Deadwood-Dependent (Saproxylic) Invertebrates

Our focal invertebrate taxa comprise three wood-feeding insects: a eusocial termite (*Reticulitermes flavipes* Kollar, Blattodea: Rhinotermitidae), a sub-social cockroach (*Cryptocercus punctulatus* Scudder, Blattodea: Cryptocercidae), and a beetle (*Odontotaenius disjunctus* Illiger, Coleoptera: Passalidae). Additionally, our set includes two myriapods: a top-level predatory bark centipede (*Scolopocryptops sexspinosus* Say, Scolopendromorpha: Cryptopidae), and a detritivorous round-backed millipede (*Narceus americanus* Beauvouis, Spirobolida: Spirobolidae). All five species are forest floor-dwellers associated with rotting logs (angiosperms or conifers). The wood-feeders generally excavate galleries in the sapwood and nest in the heartwood whereas the centipede is most commonly found directly beneath residual loose bark, although females brood their eggs within interior cavities of rotting logs. Although the millipede is primarily a leaf litter dweller, it often shelters underneath logs, at the soil-wood interface. All species are native to the southern Appalachians and they are believed to have a long history of co-occupancy. Given their shared dependence on the same microhabitat type, concerted responses to past environmental change are plausible (although differences in life history and other traits may lead to discordance among saproxylic invertebrates; see Sunnucks et al. 2006, Garrick et al. 2008).

Goals and Approach

In this paper, we used the extent of spatial overlap in ecological niche modeling-based estimates of historical habitat stability to generate predictions about phylogeographic congruence under a scenario where abiotic factors were the primary drivers of responses of saproxylic invertebrates to Pleistocene (and earlier) environmental change in the southern Appalachian Mountains. For comparison, we also inferred ecological co-associations among each of the five focal species using information on food web structure for southern Appalachian saproxylic invertebrates (Garrick et al. 2019a), relative arrival times during the succession that accompanies wood decomposition (Stokland et al. 2012, Messier et al. 2014), frequency of very fine-scale co-occurrence (i.e., syntopy), and proxies for interaction type (Morales-Castilla et al. 2015). This provided a basis for predicting the strength of phylogeographic congruence under a scenario in which biotic influences predominated. While we recognize that the two competing scenarios are not mutually exclusive, assessing the relative importance of historical habitat stability versus ecological co-associations is a valuable first step in understanding whether biotic interactions act as a constraint on species' responses to past environmental change. After identifying contrasting a priori predictions based on the two scenarios, we tested them by reconstructing the long-term population history of each species using mitochondrial and nuclear DNA sequence data. Four axes of comparison among species were considered: the geographic distribution of distinct spatial-genetic clusters, phylogeographic structure, changes in effective population size over time, and historical gene flow dynamics. Accordingly, our assessments

of congruence focused on the extent of spatial coincidence of breaks between clusters, the depth of divergence among intraspecific lineages, the nature of population size changes (i.e., growth vs. decline), and source-sink gene flow relationships.

Materials and Methods

Predictions Based on Historical Habitat Stability

To identify potential locations of long-term habitat refugia, we estimated paleo- and present-day ENMs for each species. Habitat stability was derived from a time series of ENMs, and the degree of overlap among each pair of species' climatic stability surfaces was then quantified. This generated a priori predictions about expected levels of phylogeographic congruence among all five species, under a scenario where abiotic factors predominate.

Species Occurrence Data

Species occurrence data were based on presence-only records compiled from our own fieldwork, published literature, and/or the Global Biodiversity Information Facility (https://www.gbif.org). Notably, molecular techniques are required for accurate species-level identification of the focal termite when only the worker caste is available, which is often the case, given that several otherwise indistinguishable congeners co-occur in the southern Appalachians and elsewhere (Garrick et al. 2015a). This constrained high-quality occurrence records for this species (see Hyseni and Garrick 2019b). To avoid introducing bias into downstream comparisons among species owing to strongly contrasting occurrence data extents, we used a 100 km buffer around the perimeter of the termite occurrence records as the limit for inclusion of occurrence records from the other four species (Supp Fig. 1 [online only]). Ultimately, the total number of non-redundant occurrence records used for estimating species-specific ENMs were: *C. punctulatus n* = 464, *R. flavipes n* = 97, *O. disjunctus n* = 320, *S. sexspinosus n* = 158 and *N. americanus n* = 243.

Selection of Climatic Variables

ENM was performed on three timescales: present-day (1960–1990), Mid-Holocene (MH; ~6 KYA), and Last Glacial Maximum (LGM; ~22 KYA). We used four environmental factors as predictors. To deal with collinearity among the 19 bioclimatic variables from WorldClim database v.1.4 (http://www.worldclim.org; Hijmans et al. 2005), these predictors were obtained via factor analysis (see Hyseni and Garrick 2019a for details). The four factors captured annual temperature range, summer temperature, dry- and wet-season precipitation and are available as raster maps at a 1-km resolution from DRYAD (Hyseni and Garrick 2020).

Ecological Niche Modeling and Projections

ENMs were estimated for each species separately using the BIOMOD2 package (Thuiller et al. 2009, Di Cola et al. 2017) in R (R Core Team 2020). We selected pseudo-absence points from outside the area predicted as suitable habitat via the rectilinear surface range envelope model. Using presence and pseudo-absence data, we ran two modeling algorithms: artificial neural networks (Ripley 1996), and random forest (Breiman 2001). We then used the ensemble framework (Buisson et al. 2010) to obtain a weighted average. For further modeling details, including assessment of model performance, see Hyseni and Garrick (2019a).

Climatic Stability and Overlap

To generate a climatic stability surface, the probability of occurrence layers for each species derived from ENMs for each time period were multiplied to obtain the areas with climatic stability (CS) across all three time periods using the equation:

$$P_{CS}(Current \cap MH \cap LGM) = P(Current) \times P(MH) \times P(LGM) \quad (1)$$

where P_{CS} is the probability of occurrence of a species in all three time periods and P is the probability of species occurrence in one particular time period. As a result, the output was a map with values ranging from 0 (i.e., focal species not predicted to be present during any time period) to 1 (i.e., focal species predicted to be present in all time periods). The CS overlap between each pair of species was calculated using Schoener's (1968) D statistic (where values ranged from 0 for no overlap, to 1 for identical climatically stable areas), implemented in the ENMEVAL package (Muscarella et al. 2014) in R. Finally, an unrooted dendrogram was used to visually represent these overlap values (where 1 – D was used to generate the dissimilarity matrix used for hierarchical clustering). Ultimately, this provided a priori predictions about phylogeographic congruence under a scenario where abiotic factors drive species' responses.

While we believe that using a100 km buffer around the perimeter of the termite occurrence records as the limit for inclusion of occurrence records reduced bias associated with how widely distributed and/or well-documented a species happens to be, we acknowledge that this may have affected the estimated ENMs and CS maps for the beetle, centipede, and millipede (the cockroach records were not cropped, and therefore unaffected), as well as Schoener's (1968) D statistic for all species pairs. Thus, for completeness, we also present the distribution of all available reliable occurrence records for each species (Supp Fig. 2 [online only]) and used these to re-estimate their ENMs and CS maps, and re-calculate D values for each species pair, although we did not use outcomes from this alternative approach for downstream hypothesis-testing.

To facilitate visualization of areas that likely served as key long-term multi-species habitat refugia, we performed a follow-up analysis. Here, the area of CS across all five species for all three time periods was calculated using the combined probabilities for each species, by applying the equation:

$$\begin{aligned} P'(Cp \cup Na \cup Od \cup Rf \cup Ss) &= P_{CS}(Cp) + P_{CS}(Na) + P_{CS}(Od) \ldots \\ &- P_{CS}(Cp \cap Na) - P_{CS}(Cp \cap Od) \ldots + P_{CS}(Cp \cap Na \cap Od) \\ &+ P_{CS}(Cp \cap Na \cap Rf) \ldots - P_{CS}(Cp \cap Na \cap Od \cap Rf) \\ &- P_{CS}(Cp \cap Na \cap Od \cap Ss) \ldots + P_{CS}(Cp \cap Na \cap Od \cap Rf \cap Ss) \end{aligned} \quad (2)$$

where P' is the combined probability for all species in all three time periods, P_{CS} is the CS of each species obtained using equation 1, and abbreviations for species names are as follows: *Cp* (*C. punctulatus*), *Rf* (*R. flavipes*), *Od* (*O. disjunctus*), *Ss* (*S. sexspinosus*) and *Na* (*N. americanus*). As a result, we created an output map with values ranging from 0 (i.e., stable habitat not predicted to be present during any time period for any species) to 1 (i.e., stable habitat predicted to be present in all time periods for all species). To calculate equation 1 and 2 probabilities, the RASTER package (Hijmans 2020) in R was used. As above, for exploratory purposes, we also re-generated a map of long-term multi-species habitat refugia based on all available reliable occurrence records for each of the focal species.

Predictions Based on Ecological Co-associations

We considered four components of actual or potential direct interactions among species: trophic guild (i.e., similar exploitation of the same class of resource, sensu Simberloff and Dayan 1991), the timing of colonization during succession, frequency of very fine-scale co-occurrence (i.e., syntopy), and interaction type inferred from traits (Morales-Castilla et al. 2015). For all species pairs, each of the four components was represented as a dissimilarity matrix (Supp Table 1 [online only]), and then hierarchical clustering was used to represent these as unrooted dendrograms.

Trophic Guild

Garrick et al. (2019a) estimated the basic food web structure of southern Appalachian saproxylic invertebrates, which we used as our framework here. Briefly, the cockroach (*C. punctulatus*), termite (*R. flavipes*) and beetle (*O. disjunctus*) are all wood-feeders occupying the same guild, such that dissimilarity among them was scored as 0. The millipede (*N. americanus*) is also a primary consumer, but it is a detritivore that mostly feeds on decaying leaves (Walker et al. 2009). Compared to the wood-feeders, this lateral separation in the food web was given a dissimilarity score of 1. The centipede (*S. sexspinosus*) is a top-level (i.e., tertiary) generalist predator that feeds on insects, spiders, and worms, as well as other centipedes (Auerbach 1951). Owing to the two levels of vertical separation in the food web relative to the primary consumers, pairwise species comparisons that included the centipede were assigned a score of 2.

Timing of Colonization

Given that most saproxylic invertebrate species use rotting logs at specific stages of decay, patterns of succession are predictable (Messier et al. 2014). In temperate forests of the eastern United States, a newly fallen dead tree is usually first colonized by fungi, transferred by wood-boring bark beetles. Next, aided by moderate powers of dispersal, termites and their predators arrive at intermediate stages when cellulose and lignin have begun to break down and the outer bark has loosened. The tunneling activities of termites create galleries in the sapwood and modify substrate properties, facilitating subsequent colonization of large-bodied wood-feeding insects. At the most advanced decay stages, leaf litter-dwelling invertebrates seeking shelter can opportunistically occupy larger tunnels (Stokland et al. 2012, Ulyshen 2016, Brin and Bouget 2018). Accordingly, we assigned relative arrival times to each species (early: termite and centipede, intermediate: cockroach and beetle; late: millipede) and scored timing of colonization during succession as concurrent (0), sequential (1), or highly asynchronous (2).

Frequency of Syntopy

In addition to the opportunistic sampling of the five focal species from 219 rotting logs to obtain tissue for phylogeographic analyses (see *Population Sampling and Genetic Screening* below), we also conducted exhaustive community-level surveys in Bankhead National Forest, Alabama, and Great Smoky Mountains National Park, Tennessee and North Carolina. For these surveys, 22 mid- to late-stage rotting logs were fully dismantled, with all macroscopic arthropods collected (Garrick et al. 2019a). This generated a dataset of 241 logs that provided information on the frequency of syntopy among the five species that we focus on in the present study. Given that there was considerable asymmetry in the number of occurrences per species (e.g., 139 logs containing the cockroach versus 20 with the millipede), calculations were conditioned on the rarest species in a pair (e.g., for three cockroach-millipede co-occurrences, the observed frequency was 3/20). To convert this into a dissimilarity score, the observed frequency was subtracted from one (e.g., 1 – 0. 15 = 0.85). For consistency with our scoring regime for the other components of actual or potential direct interactions among species (i.e., trophic guild, etc.), the aforementioned dissimilarity scores were rescaled to range from 0 to 2 (continuous values).

Interaction Type

We considered six types of species interaction (Brin and Bouget 2018), and based our inferences on proxies that included morphological and behavioral traits, as well as the available information on trophic guilds and succession. There were four clear predator/prey interactions (+/–), with the centipede as the beneficiary in all cases. Also, there were four probable commensalistic interactions (0/+): two involved facilitation of the cockroach and beetle by the primary gallery-forming activities of the termite, and the other two were based on the facilitation of the millipede by secondary gallery-forming activities of the cockroach and beetle. We identified only one likely case of competition (–/–) between the cockroach and beetle owing to their membership in the same trophic guild coupled with approximately synchronous arrival time during succession. Ecological neutrality (0/0) also seemed limited to one species pair (i.e., the termite and millipede, given their different trophic guilds and highly asynchronous arrival). We did not identify any potential cases of mutualism (+/+) or amensalism (–/0). To represent the four inferred interaction types as dissimilarity scores, we tallied the total count of antagonistic (–) interactions (i.e., 0 for neutral or commensalism, 1 for predator/prey, and 2 for competition).

Given that the characterization of species interactions is notoriously difficult in the absence of controlled experiments, even for a relatively modest number of species (e.g., Carrara et al. 2015, Dormann et al. 2018), we augmented the above approach by re-assessing the nature and strength of putative associations using checkerboard analyses (Stone and Roberts 1990) performed with the ecospat package (Di Cola et al. 2017) in R. As a measure of species co-occurrence, the *C*-score has been shown to have good statistical power for detecting non-randomness (Gotelli 2000). The checkerboard analysis is based on co-occurrence data and quantifies the extent to which two species repel one another (a *C*-score higher than expected by chance is indicative of a strongly antagonistic interaction such as competition, –/–) or aggregate together (a *C*-score lower than expected by chance is indicative of a positive interaction such as mutualism, +/+). In cases where there is no significant difference between observed and expected *C*-scores (i.e., a random pattern of co-occurrence), then no direct interaction (i.e., ecological neutrality; 0/0) is inferred. We used occurrence data at the level of individual sampling sites (i.e., logs with the same coordinates pooled; Supp Table 2 [online only]) and simulated "control groups" representing random colonization and co-occurrence patterns (i.e., null distributions of expected *C*-scores) were constructed in two ways: unconstrained matrices, and environmentally constrained matrices. Whereas the former approach makes no distinction between a species occurrence in a peripheral versus core part of its range and therefore does not consider implications for local abundance, the latter uses habitat suitability as site weights to further constrain simulations of the control group (see Di Cola et al. 2017). Here, we used habitat suitability scores derived from the present-day ENMs (described under *Predictions based on historical habitat stability,* above) as the environmental constraints, and used 10,000 permutations to generate matrices for the null models.

Since the degree of "checkerboardedness" is informative only about balanced interactions (cf., the six types considered above), outcomes were interpreted as being confirmatory only.

Synthesis of Components

Ultimately, predictions about phylogeographic congruence under a scenario in which biotic influences predominate were generated by combining all four components of ecological co-associations. Equal weighting was attributed to each; given that all dissimilarity scores ranged from 0 to 2, these were simply summed across the four matrices. Hierarchical clustering was then performed, and an unrooted dendrogram was generated. To assess robustness of the final four-component predictions, we used a "leave-one-out" approach to create four jackknife replicates (i.e., each with a different combination of three components of ecological co-associations), reanalyzed them, and then visually assessed topological agreement among the dendrograms.

Population Sampling and Genetic Screening

From 2012 to 2017, specimens were opportunistically collected from 219 rotting logs throughout forests in the southern Appalachian Mountains and surrounding areas, across eight states. This was conducted under scientific collecting permits issued by the Alabama Department of Conservation and Natural Resources, Georgia Department of Natural Resources (permit 29-WBH-12–16), United States Department of Agriculture Forest Service, and United States National Park Service (permits GRSM-2012-SCI-2242, SHEN-2012-SCI-0015, and CUGA-2012-SCI-0008). Sampling included logs at mid- to late stages of decomposition in hardwood, pine, and mixed forests. Specimens of the five focal species obtained from community-level surveys (Garrick et al. 2019a) were included in the present dataset. All samples were stored in 95% ethanol. Representatives will be lodged at the Mississippi State University entomological collection following completion of on-going projects still using them. We also included Swanson's (2005) geo-referenced mitochondrial DNA sequence data for 18 individuals of the focal beetle species sampled from the southern Appalachian Mountains (see Garrick et al. 2019b for details on sequence trimming, and integration). Ultimately, all invertebrate samples with molecular data came from 230 rotting logs (Supp Table 2 [online only]).

Genomic DNA was extracted from whole specimens (*R. flavipes*) or legs (all other taxa) using a DNeasy Blood and Tissue Kit (Qiagen, Valencia CA, USA), following the manufacturer's recommendations. For each species, one mitochondrial DNA (mtDNA) and one nuclear DNA (nDNA) locus was targeted. Conditions for polymerase chain reaction (PCR) amplification of portions of mtDNA cytochrome oxidase subunit I (*COI*) and/or subunit II (*COII*) genes for *C. punctulatus*, *R. flavipes*, *S. sexspinosus*, and *O. disjunctus* are reported elsewhere (Garrick 2016; Garrick et al. 2015a, 2018, 2019b, respectively). For *N. americanus*, a mtDNA region spanning 16S rRNA, $tRNA^{Val}$, and 12S rRNA was amplified following Walker et al. (2009). Conditions for amplification of some nuclear loci, including histone (*H3A*) for *C. punctulatus*, an intronic portion of nuclear gene endo-beta-1,4-glucanase (*EB14G*) for *R. flavipes*, and RNA polymerase subunit 2 (*RNP2*) for *S. sexspinosus*, have been published (Inward et al. 2007, Garrick et al. 2018, Hyseni and Garrick 2019a, respectively). Newly developed primers used to amplify *H3A* for *O. disjunctus* and internal transcribed spacer 2 (*ITS2*) for *N. americanus* are reported in Supp Table 3 [online only]. PCR products were viewed following electrophoresis, purified using ExoSAP-IT (Affymetrix, Santa Clara, CA, USA), and sequenced on an Applied Biosystems 3730x Genetic Analyzer at Yale University. Chromatograms were edited and aligned in MEGA v6.06 (Tamura et al. 2013) or GENEIOUS v.6.1.8 (Kearse et al. 2012). All geo-referenced genetic datasets analyzed in this paper are available via DRYAD Repository entry https://doi.org/10.5061/dryad.pvmcvdnkd.

To confirm that data from true mtDNA had been obtained (cf., nuclear pseudogenes), *COI* and *COII* sequences were translated into amino acids, and all sequenced regions were compared to accessions in NCBI's nucleotide database via BLAST searches (Altschul et al. 1990). Heterozygous sites in nDNA alignments were coded using IUPAC ambiguity codes when the height of the secondary peak was at least 50% that of the primary peak. Gametic phase of segregating sites in multi-site heterozygotes was computationally inferred using the PHASE algorithm (Stephens et al. 2001), implemented in DNASP v.6.12.03 (Rozas et al. 2017). Run settings for reconstruction of nDNA allele haplotypes followed Hyseni and Garrick (2019a). To avoid introducing downstream systematic bias, individuals with low-confidence haplotype pairs were retained (Garrick et al. 2010). For each species, evidence for intra-locus recombination among phased nDNA alleles was assessed with RDP v.4.100 (Martin et al. 2015), using the following suite of methods that do not require non-recombinant reference sequences: Geneconv (Sawyer 1989), MaxChi (Maynard Smith 1992), Bootscan (Salminen et al. 1995), RDP (Martin and Rybicki 2000), and Chimaera (Posada and Crandall 2001).

Genetic Data Analyses Used to Assess Predictions

Comparative phylogeography faces the challenge of assessing congruence, despite some level of the inherent idiosyncrasy of species' responses to past environmental change. That is, the parameter space of potential paths to incongruence is much larger than that leading to congruence. Accordingly, we simplified our assessment to consider four axes of comparison: the distribution of natural spatial-genetic clusters, phylogeographic structure, changes in effective population size over time, and historical gene flow dynamics. Although this approach necessarily sacrifices detail for an overarching pattern, it does provide a useful framework for minimizing potential bias toward inferring incongruence (Burgess and Garrick 2020).

Natural Spatial-Genetic Clusters

The number of geographically cohesive genetic groups within each species was inferred using individual-based spatial clustering of mtDNA sequence data, analyzed using BAPS v.6.0 (Cheng et al. 2013). For *C. punctulatus*, *R. flavipes* and *O. disjunctus*, a concatenated dataset comprised of mtDNA *COI*+*COII* was used because these genes are effectively part of the same locus (no concatenation was necessary for *S. sexspinosus* and *N. americanus*, as their mtDNA regions were sequenced in a single continuous read). Given that two or more individuals with different mtDNA haplotypes were sometimes collected from the same location, for each species, we crated eight sub-sampled datasets in which only one haplotype per spatial coordinate was included per dataset. Across these eight replicates, all unique haplotypes from a given location were represented at least once. This approach was used (cf., randomly perturbing spatial coordinates) to avoid artificially increasing the complexity of Voronoï tessellations. For *C. punctulatus*, *R. flavipes*, *O. disjunctus* and *S. sexspinosus*, we assessed values of *K* (i.e., the number of clusters) ranging from 1 to 20, whereas for *N. americanus*, the maximum *K* was set at 16 (i.e., the total number of unique sampling

site coordinates for this species). In all cases, the best-fit K was identified via log marginal likelihood scores. To quantify levels of polymorphism, DNASP was used to calculate the number of unique haplotypes (N_{hap}), number of segregating sites (S), and nucleotide diversity (π) for mtDNA and nDNA loci. For each species, these statistics were calculated separately for each BAPS cluster, and for all clusters combined.

Congruence Assessment

Due to highly heterogeneous geographic sampling per species, statistical testing of spatial coincidence of breaks between clusters (e.g., using boundary overlap statistics) was not feasible. Accordingly, here we relied on visual assessment.

Phylogeographic Structure

To understand whether divergence among intraspecific BAPS clusters occurred over relatively short timescales (i.e., attributable to drift alone) versus longer phylogeographic timescales (i.e., over which nucleotide mutations accumulate), following Garrick et al. (2004) we directly compared partitioning of genetic variation in mtDNA datasets, and nDNA datasets, using Weir and Cockerham's (1984) F_{ST} versus Excoffier et al.'s (1992) Φ_{ST}. When calculating Φ_{ST}, the best fit model of molecular evolution was first determined from DNA sequence alignments using jModelTest 2 v.2.1.6 (Darriba et al. 2012), and then a maximum likelihood-corrected genetic distance matrix was generated using PAUP* v.4.0a (Swofford 2003). F_{ST} versus Φ_{ST} values were estimated in ARLEQUIN v. 3.5.2.2 (Excoffier and Lischer 2010), with significance (α = 0.05) assessed via 999 permutations.

To further assess whether intraspecific BAPS clusters were evolutionarily distinct, we estimated phylogenetic relationships among mtDNA haplotypes from each species using maximum likelihood. To identify the optimal partitioning scheme and models of evolution, we evaluated each dataset with PARTITIONFINDER v2.1.1 (Lanfear et al. 2017) using the greedy algorithm, linked branch lengths, and model selection using the corrected Akaike information criterion (AICc; Hurvich and Tsai 1989). For *C. punctulatus*, *R. flavipes,* and *O. disjunctus,* we provided six possible partitions, corresponding to each codon position of the two mtDNA genes. Given that only one mtDNA gene was sequenced *S. sexspinosus*, we ran PARTITIONFINDER with three possible partitions, with all other settings as above. For *N. americanus*, we ran three possible partitions, one for each of the non-protein coding genes:16S rRNA, Valine-encoding tRNA, and 12S rRNA. For each partitioning scheme, we evaluated three models of evolution: generalized time-reversible model (GTR; Tavaré 1986), GTR+G, and GTR+G+I. To obtain a single model for tree inference, albeit with independent model parameter values, we first identified the best partitioning scheme for each of the three models of evolution based on AICc values. We then compared the AICc of the best partitioning scheme for each of the three models and selected the partitioning scheme and evolutionary model combination with the lowest AICc score. Phylogenetic relationships were inferred using RAxML v.8.2.1.1 (Stamatakis 2014). For each mtDNA dataset, we used the partitioning scheme and evolutionary model identified by PARTITIONFINDER. Each partition identified by PARTITIONFINDER was allowed an independent implementation of the best model. Node support was assessed using 1,000 bootstrap pseudo-replicates. For each species, the most closely related taxon with publicly available sequence data for the corresponding mtDNA region(s) was used as an outgroup (Supp Table 4 [online only]).

Congruence Assessment

Our first comparison across species was based on the *depth of phylogeographic structure*. Here, if Φ_{ST} values clearly exceeded corresponding F_{ST} values over all pairs of BAPS clusters for both mtDNA and nDNA, this was considered indicative of ancient divergence among intraspecific lineages (i.e., deep phylogeographic structure). Conversely, $\Phi_{ST} > F_{ST}$ for mtDNA only would suggest more recent divergences (i.e., moderate phylogeographic structure), and $\Phi_{ST} \approx F_{ST}$ for both mtDNA and nDNA would be consistent with very shallow (or a lack of) phylogeographic structure. Our second type of comparison was based on *topological phylogeographic structure*. Here, for each species, mtDNA-based phylogenetic relationships among members of BAPS clusters were compared to the spatial location of those same clusters. If the RAxML tree topology strongly corresponded with geography (i.e., sister lineages were also geographic neighbors), the species was categorized as displaying strong topological phylogeographic structure. Conversely, if phylogenetic and geographic relationships required reconciliation via invoking one or more major long-distance dispersal events to explain non-neighboring sister lineages, this was considered a weak topological phylogeographic structure.

Changes in Effective Population Size Over Time

To assess evidence for changes in effective population size (N_e) over time (or lack thereof), for each BAPS cluster we calculated Fu's (1997) F_S, Tajima's (1989) D, Ramos-Onsins and Rozas's (2002) R_2, and Harpending's (1994) r for mtDNA and nDNA separately, in DNASP. Deviations from the null hypothesis of population size constancy were evaluated by comparing observed values against distributions simulated via neutral coalescence (1,000 replicates), with significance assessed at the α = 0.05-level (except for F_S, where α = 0.02 was used, following Fu 1997). Population growth was inferred from significantly negative F_S or D, and from significantly small R_2 or r. Conversely, the decline was inferred from significantly positive F_S or D, and significantly large R_2 (r is not informative about decline, since ragged multi-modal mismatch distributions are also expected under long-term stability).

We also examined signatures of historical population size change for each BAPS cluster using extended Bayesian skyline plots (EBSP; Heled and Drummond 2008), implemented in BEAST v.2.6.2 (Bouckaert et al. 2019). Separate searches were performed for single-locus datasets using relatively simple substitution models (i.e., Hasegawa et al.'s [1985] HKY with empirical base frequencies for mtDNA, and Jukes and Cantor's [1969] JC for nDNA, respectively), and for multi-locus datasets with ploidy of each locus specified via the inheritance scaler. Settings were: clock model = strict, clock rate = 1 (i.e., time measured in substitutions, with mtDNA as the reference in multi-locus analyses), operator weights = auto-optimized (following Heled 2016), with other priors as default. Depending on the dataset, final searches were performed using either 2.0×10^7, 5.0×10^7, or 1.0×10^8 Markov chain Monte Carlo (MCMC) generations, sampling parameters every 5,000th or 10,000th step (with 10% discarded as burn-in). Convergence of chains was assessed via effective sample size (ESS) values for key demographic parameters calculated using TRACER v.1.7.1 (Rambaut et al. 2018), and by comparing outcomes from independent runs. We required ESS >200 for reliable inference (otherwise, no attempt to interpret the EBSP was made). Two or three replicate runs were pooled to estimate the median and 95% highest posterior density (HPD) credible set of values for the "number of population size changes" parameter. If the median was >0, then the programs LOGCOMBINER and EBSPANALYSER

within the BEAST package were used to generate EBSP curves: the directionality of size change (i.e., growth vs. decline) was determined via visual assessment of trends in median N_e over time, relative to upper and lower bounds of the 95% HPD of N_e.

Given the contrasting sensitivities of different demographic summary statistics (Ramos-Onsins and Rozas 2002) and the potential for overinterpretation of EBSPs (Heller et al. 2013), we adopted a conservative interpretative framework. Following Garrick et al. (2015b), historical population size change was inferred only when at least two different analyses of the same DNA sequence dataset supported either growth or decline (i.e., corroboration across loci was not required), and there was no strong conflict among different analyses. Otherwise, the null hypothesis of stable population size was retained. Ultimately, growth was interpreted as evidence for post-glacial expansion, whereas decline was considered indicative of habitat contraction and/or fragmentation during cool dry glacial periods. Outcomes from multi-locus EBSPs were considered as confirmatory only (cf., being a stand-alone source of potentially novel demographic inference).

Congruence Assessment

To simplify comparisons across species, we considered the nature of past population size changes (i.e., growth vs. decline) or lack thereof (i.e., long-term stability) in each of two major partitions of the study area: the northern region, and the southern + central region. This geographically based partitioning helped accommodate differences in the number and distribution of natural spatial-genetic clusters (i.e., there were several cases of "no-analog" species-specific BAPS clusters). Given the considerable among-species spatial coincidence of breaks between predominantly northern versus southern + central BAPS clusters (see Results), the chosen level of regional coarseness avoided arbitrary boundary placement. Ultimately, each species was classified as having a history of growth, decline, or stability in the northern region, and likewise, growth, decline, or stability in the southern + central region. Cross-validated single-locus inferences for the BAPS cluster(s) occupying a given region—regardless of which locus or how many loci these were based on—determined which of the three demographic "states" was assigned.

Historical Gene Flow Dynamics

To identify the location(s) of key habitat linkages that served as gene flow conduits and refuges that acted as sources of recolonization into neighboring areas, we estimated a maximum likelihood gene flow matrix for each species using MIGRATE v.3.6.11 (Beerli and Felsenstein 2001). This method estimates θ (N_e. μ for mtDNA or $4N_e$. μ for nDNA, where μ is the mutation rate) and M (migration rate per generation divided by μ). Following Garrick et al. (2008), we implemented a two-tiered hypothesis-testing approach. Initially, likelihood-ratio tests (LRTs) were used to assess significance ($\alpha = 0.05$) of departure from the null hypothesis of complete genetic isolation between pairs of BAPS clusters ($M_{1\rightarrow2} = M_{2\rightarrow1} = 0$). For each species, all possible pairs of clusters were evaluated using separate LRTs. Wherever $M = 0$ could not be rejected, this indicated that the full matrix could be reduced to exclude these connections. Next, we assessed the significance of departure from the null hypothesis of symmetrical gene flow ($M_{1\rightarrow2} = M_{2\rightarrow1}$), again with all pairs of BAPS clusters evaluated using separate LRTs. Search settings were: 10 short MCMC chains (5.0×10^3 steps), three long chains (5.0×10^4 steps) recording every 100th genealogy, a 50,000-genealogy burn-in per chain, MC^3 heating (temperatures: 1.0, 1.5, 2.5, and 4.0), UPGMA starting trees, empirical base frequencies and a transition/transversion ratio of 2. Initial values for θ and M were set using F_{ST}, and all parameter estimates were generated by combining five replicate runs. DNA sequences were analyzed as single-locus datasets. All MIGRATE runs (and associated LRTs) were repeated five times. Based on these replicate runs, a consensus vote approach was used was to make final inferences about genetic isolation, or symmetry of gene flow. In cases of significant asymmetry, source-sink relationships were characterized using point estimates of M, again using a consensus vote.

Congruence Assessment

We focused on two components of estimated gene flow matrices. First, for each species, the BAPS cluster that had the greatest number of significant gene flow connections (i.e., those for which $M > 0$, $P > 0.05$), irrespective of directionality, was identified as the *hub of connectivity*. These clusters represent geographic locations that act as conduits for gene flow, without which, genetic isolation would be elevated considerably. Second, we identified *source-sink relationships*. Here, we defined sources as clusters with a predominance of emigration exceeding immigration (i.e., $M \neq s$, $P > 0.05$, in the direction of outgoing gene flow), consistent with expectations for refugial areas that were sources of recolonization elsewhere. Conversely, clusters that were predominantly recipients of significantly asymmetric gene flow were identified as sinks. Thus, primary comparisons were based on each species being classified as having versus lacking a hub of connectivity, and having versus lacking source-sink relationships. Secondarily, we considered geographic concordance, for which we relied on visual assessment. In all cases, mtDNA versus nDNA inferences were considered separately.

Results

Predictions Based on Historical Habitat Stability

ENMs showed that suitable habitats for *C. punctulatus* were predicted to have been narrowly distributed during the LGM, limited to high elevation montane areas, but then progressively expanded to include mid-elevation areas in the MH and present-day (Fig. 1). While similar dynamics were indicated for *R. flavipes*, compared to the cockroach, this species appears to have been somewhat less restricted during the LGM, and the extent of post-LGM expansion was greater. This was also reflected by the CS maps for these two taxa. Suitable habitats for the other three species were predicted to have distributions that closely matched one another in the LGM; subsequent expansion in the MH and the present-day also showed similar trajectories, albeit with some species-specific differences, particularly for the CS maps. Nonetheless, *O. disjunctus*, *S. sexspinosus* and *N. americanus* appeared to have relatively broad potential ranges over time, whereas the cockroach and termite were more geographically restricted (Fig. 1; ENMs and CS maps recalculated using all available reliable occurrence records are shown in Supp Fig. 3 [online only]). Outcomes from the quantitative comparison of CS overlap among species (Supp Table 5 [online only]) showed that *C. punctulatus* and *R. flavipes* were predicted to have the most similar phylogeographic histories. These species form a clearly separated group on the dendrogram based on Schoener's (1968) *D*. The other three species formed a second major group, within which *O. disjunctus* and *N. americanus* were most similar (Fig. 2, left panel; exploration of impacts of using uncropped occurrence records showed that the two major groups remained unchanged, but dendrogram-based relationships within the three species group did differ; see Supp Table 6 and Fig. 4 [online only]). Follow-up analysis

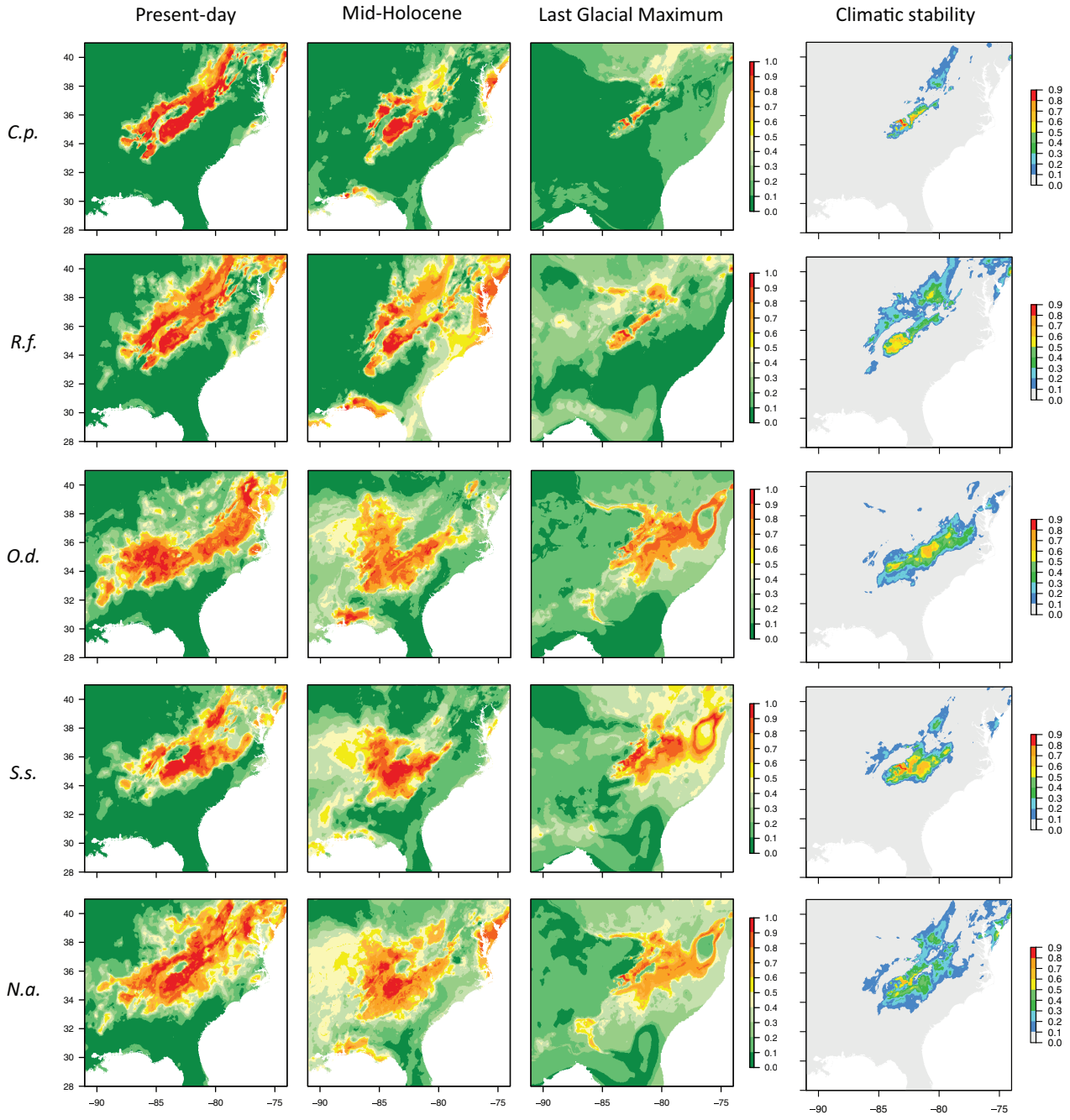

Fig. 1. Ecological niche models (ENMs) estimated for each of the five species from present-day to Last Glacial Maximum, and climatic stability based on the ENM time series. Color coding uses "warm" colors to indicate areas of highest probability of occurrence, or highest climatic stability. Species names are abbreviated as follows: *C.p.* (*Cryptocercus punctulatus*), *R.f.* (*Reticulitermes flavipes*), *O.d.* (*Odontotaenius disjunctus*), *S.s.* (*Scolopocryptops sexspinosus*), and *N.a.* (*Narceus americanus*).

of areas that likely served as key long-term multi-species habitat refugia indicated that all five species persisted in situ and/or near the southern Appalachians, and thus are likely to have had long-term ecological co-associations (Supp Fig. 5 [online only]; the same pattern and associated inference held true when this projection was based on all available occurrence records; see Supp Fig. 6 [online only]).

Predictions Based on Ecological Co-associations

Based on a combination of four components of ecological co-associations, the three wood-feeders were predicted to show phylogeographic congruence, with the beetle and termite expected to exhibit the most similar responses to past environmental change. Conversely, the centipede was predicted to have a very unique phylogeographic history, as was the millipede, albeit to a lesser extent (Fig. 2, right panel). These predictions were quite robust: the grouping of the three wood-feeders was supported by two (50%) jackknife replicates, as was the "sister" relationship between the beetle and termite. Likewise, the distinctiveness of the centipede's history was supported by three (75%) jackknife replicates (separate dendrograms for each component of ecological co-associations are shown in Supp Fig. 7 [online only]).

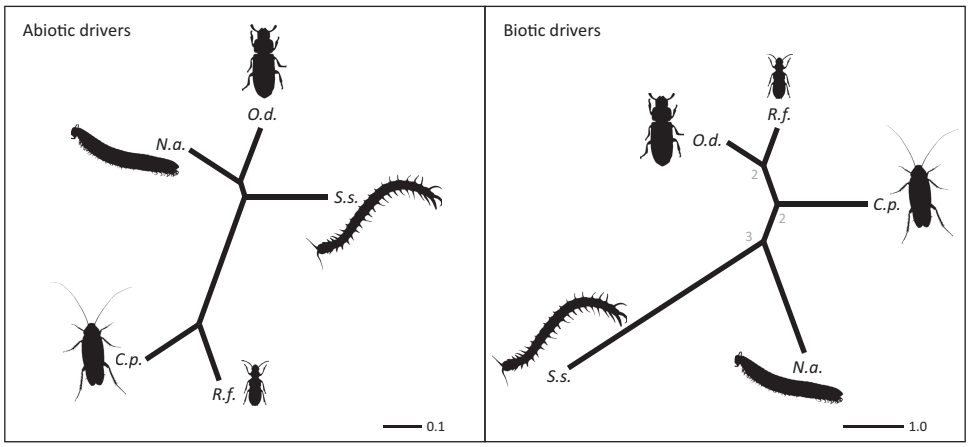

Fig. 2. Unrooted dendrograms representing two competing hypotheses about key drivers of phylogeographic congruence among five saproxylic invertebrates: abiotic factors related to historical climatic stability (left) versus biotic factors related to ecological co-associations (right). Scale bars represent either the inverse of a measure of habitat overlap (1 – Schoener's *D*; left), or the cumulative dissimilarity score for species interactions based on trophic guild, timing of colonization during succession, frequency of syntopy, and presumed interaction type (right). Numbers on nodes for the biotic drivers scenario indicate the number of jackknife replicates (out of 4) that supported a given predicted partition. Species names are abbreviated as in Fig. 1.

Regarding the "interaction type" component (see Methods) only, the unconstrained checkerboard analysis supported the notion that the beetle and cockroach had the most strongly antagonistic (i.e., repelling) interaction type, and that the beetle and termite had a positive (i.e., aggregating) interaction (see Supp Table 1 [online only] vs. Supp Table 7 [online only], top). However, the environmentally constrained *C*-scores showed several departures from proxy-based inferences (see Supp Tables 1 vs. 7 [online only], bottom). Thus, corroboration of our primary inferences about interaction type was somewhat equivocal, suggesting that cautious interpretation is warranted.

Population Sampling and Genetic Screening

Sequence data from 701 invertebrate specimens were analyzed. Sample sizes and geographic coverage ranged from 40 individuals across 16 sites (*N. americanus* nDNA) to 286 individuals across 113 sites (*C. punctulatus* mtDNA). MtDNA sequence data were obtained for all specimens included in this study, and alignment lengths ranged from 632-bp (*S. sexspinosus*) to 1125-bp (*C. punctulatus*). There was no evidence for nuclear mitochondrial pseudogenes. On average, 90% of individuals per species also had nDNA data (range: 83–98%), for which alignment lengths ranged from 251-bp (*R. flavipes*) to 879-bp (*S. sexspinosus*; Supp Table 8 [online only]). Although some nDNA regions are likely multi-copy (e.g., ITS2), within individuals, patterns of variation at heterozygous sites were consistent with single-copy diploid loci, enabling computational phasing. There were no signatures of intra-locus recombination among phased alleles.

Genetic Data Analyses Used to Assess Predictions

Natural Spatial-Genetic Clusters

Outcomes from BAPS analyses were consistent across replicate datasets. The best-fit number of clusters differed for each species, ranging from $K = 1$ (*O. disjunctus*) to $K = 6$ (*C. punctulatus*; Fig. 3). Within each species, all individuals from a given sampling site had the same cluster membership, with one exception: members of two *N. americanus* clusters ("A" and "D") were sampled from the same rotting log (i.e., A20; see Supp Table 2 [online only]). Although spatial projections of BAPS clusters are not directly comparable across species owing to differences in the underlying Voronoï tessellations, three features are notable. First, clusters are generally spatially cohesive and have small geographic ranges (although there is some minor disjunction/rare long-distance dispersal evident for *R. flavipes* and *N. americanus*, and *S. sexspinosus* includes a broadly distributed cluster). Second, *C. punctulatus*, *R. flavipes* and *N. americanus* each have clusters that are restricted to the northern region. Third, *C. punctulatus* and *N. americanus* contain clusters that are locally endemic to the central region (Fig. 3). Of the metrics used to quantify levels of polymorphism within each BAPS cluster, π is least sensitive to sample size differences, and so we focus on it here. Based on mtDNA (i.e., the most information-rich locus), *C. punctulatus* cluster "A" is clearly the most genetically depauperate. Only *S. sexspinosus* exhibited concordance across loci in terms of identification of the most genetically diverse cluster based on π (Table 1).

Congruence Assessment

Indications of a three-species "phylogeographic break hotspot" (sensu Rissler and Smith 2010) shared by *C. punctulatus*, *R. flavipes* and *N. americanus* is inconsistent with predictions of the historical habitat stability scenario (Fig. 2, left panel). Although there is potentially more agreement with predictions of the ecological co-associations scenario, given the closer expected similarity of the millipede to the cockroach and termite (Fig. 2, right panel), it is imperfect. Indeed, the species-specific absence of distinct clusters within *O. disjunctus* represents discordance with predictions of both scenarios.

Phylogeographic Structure

Comparisons of F_{ST} versus Φ_{ST} indicated a clear mtDNA-based phylogeographic structure for each of the four species with multiple BAPS clusters (Fig. 4). Considering mean values across all pairs of clusters per species, the magnitude by which Φ_{ST} exceeded the corresponding F_{ST} value was greatest for the millipede (12.2×), and it was also large (4.6–5.3×) for the other three species (all Φ_{ST} values were significant, $P < 0.001$). Analogous comparisons based on nDNA showed clear phylogeographic structure (1.5–8.0×) for the cockroach, centipede, and millipede, but not for the termite, where it was essentially non-existent (1.1×). Considering outcomes for both loci and the criteria described in Methods, *C. punctulatus*,

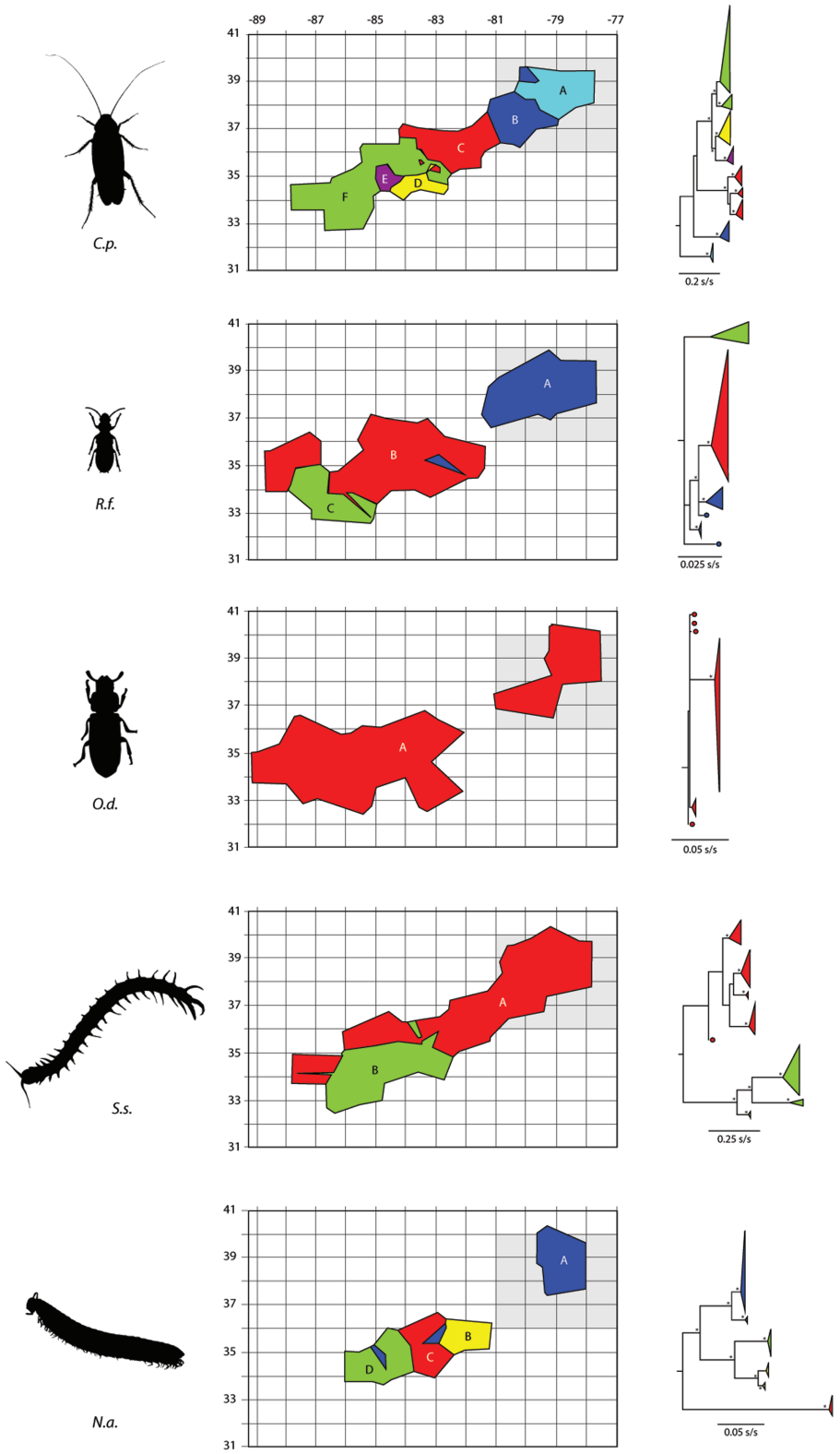

Fig. 3. The number and distribution of spatial-genetic clusters, and phylogenetic relationships among mitochondrial DNA (mtDNA) haplotypes, for each of the five focal species. BAPS clusters were arbitrarily color-coded (alphabetic names are also shown), and spatial projections were based on membership of geo-referenced individuals (Voronoï tessellations not shown). Grey shading identifies the "northern region" of the study area, referred to in the main text. Rooted phylogenetic trees (outgroup not shown) are simplified and color-coded corresponding to BAPS cluster membership of each mtDNA haplotype. Nodes with bootstrap support values >70% are marked by asterisks. Species names are abbreviated as in Fig. 1.

S. sexspinosus and *N. americanus* exhibited deep phylogeographic structure, *R. flavipes* had moderate phylogeographic structure, and *O. disjunctus* showed none (F_{ST} vs. Φ_{ST} comparisons for all pairs of clusters per species are shown in Supp Fig. 8 [online only]).

With few exceptions, mtDNA haplotypes within each BAPS cluster formed a well-supported monophyletic clade (Fig. 3; also see Supp Fig. 9 [online only] for full details). The *C. punctulatus* phylogeny showed five major clades, one of which was further divided

Table 1. Levels of DNA sequence polymorphism within each BAPS cluster, for each of the five focal species. The number of the sequenced diploid individuals (N_{indiv}) were partitioned by spatial-genetic clusters inferred using BAPS (lettered), or unpartitioned ("All"). For each locus, values of the following three summary statistics are reported: number of unique haplotypes (N_{hap}), segregating sites (S), and nucleotide diversity (π). Species names are abbreviated as in Fig. 1

		Mitochondrial DNA				Nuclear DNA			
Species	BAPS cluster	N_{indiv}	N_{hap}	S	π	N_{indiv}	N_{hap}	S	π
C.p.	A	55	9	10	0.0006	51	14	15	0.0022
	B	23	9	32	0.0051	23	5	7	0.0040
	C	50	23	125	0.0288	48	3	2	0.0004
	D	31	15	78	0.0223	31	8	5	0.0026
	E	20	8	46	0.0136	20	8	5	0.0038
	F	107	44	139	0.0178	106	25	13	0.0042
	All	286	108	322	0.0646	279	63	34	0.0105
R.f.	A	39	9	33	0.0079	31	5	4	0.0048
	B	103	19	24	0.0025	96	4	4	0.0059
	C	16	4	32	0.0113	16	4	5	0.0053
	All	158	32	86	0.0104	143	7	6	0.0062
O.d.	A (All)	133	26	42	0.0079	110	17	9	0.0074
S.s.	A	63	21	85	0.0301	59	28	50	0.0075
	B	18	13	99	0.0457	12	16	54	0.0147
	All	81	34	146	0.0570	71	44	119	0.0207
N.a.	A	25	15	29	0.0046	22	15	11	0.0045
	B	7	5	14	0.0059	7	6	6	0.0036
	C	4	4	5	0.0025	4	4	3	0.0027
	D	7	5	3	0.0010	7	7	5	0.0027
	All	43	29	181	0.0533	40	24	14	0.0061

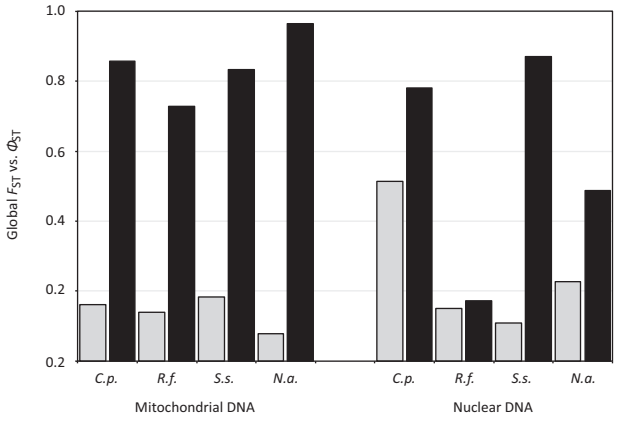

Fig. 4. Assessment of phylogeographic structure via comparison of F_{ST} (grey bars) versus Φ_{ST} (black bars). All values represent mean differentiation across all pairs of BAPS clusters per species (i.e., "global" values). Species names are abbreviated as in Fig. 1.

into two spatially proximate and narrowly distributed subclades, each representing a different BAPS cluster. Furthermore, the tree suggested a strict north to south geographic series (i.e., early to late branching). Thus, the cockroach exhibited a strong topological phylogeographic structure. For *R. flavipes*, two BAPS clusters are each monophyletic (although one has only moderate bootstrap support). However, the northern region cluster is paraphyletic, and the cluster predominantly from the central region appears to be descended from it. This suggests at least some long-distance dispersal (e.g., south to north to central colonization sequence; also see Hyseni and Garrick 2019a) which we, therefore, classified as weak topological phylogeographic structure. The two *S. sexspinosus* BAPS clusters correspond with quite deeply divergent clades (although one was only moderately well-supported). We classified this as a strong topological phylogeographic structure, as it satisfies the criterion of geographically neighboring sister lineages. Each of the four *N. americanus* clades were strongly supported (all bootstrap values >80%), as was a sister relationship between non-neighboring BAPS clusters, indicative of weak topological phylogeographic structure.

Congruence Assessment

Of the two competing scenarios considered, the finding that deep phylogeographic structure was shared by *C. punctulatus*, *S. sexspinosus* and *N. americanus* is perhaps most consistent with predictions based on a predominance of biotic influences (Fig. 2, right panel). However, this fit was still poor; although *R. flavipes* and *O. disjunctus* were united by shallower phylogeographic structure, the inferred depth differed between these two species. Considering strength of topological phylogeographic structure, neither scenario predicted that *C. punctulatus* and *S. sexspinosus* (or *R. flavipes* and *N. americanus*) would be congruent, to the exclusion of all other species.

Changes in Effective Population Size Over Time

The most compelling evidence for past population growth came from each of the four *N. americanus* clusters (based on either mtDNA or nDNA) that collectively span both the northern and southern + central regions of the study area, as well as the *C. punctulatus* cluster "A" (both loci; Table 2) restricted to the northern region. Signatures of past population decline were unique to *R. flavipes* clusters "B" and "C" (based on nDNA and mtDNA data, respectively) that both occupy the southern + central region. All other species and clusters showed no cross-validated deviations from the null hypothesis of population size stability. Of the multilocus EBSP analyses that did have sufficiently large ESS values to be considered further (i.e., 9 out of 16 datasets), most of them (6 out

Table 2. Assessment of signatures of past population size changes. For each BAPS cluster the following demographic history (or neutrality test) summary statistics are reported per locus: Fu's (1997) F_S; Ramos-Onsins and Rozas's (2002) R_2; Tajima's (1989) *D* and Harpending's (1994) *r*. Growth is indicated by significantly negative F_S or *D* (marked by *), and significantly small R_2 and *r* (marked by ^{S}). Decline is indicated by significantly positive F_S or *D* (marked by *), and significantly large R_2 (marked by ^{L}). Outcomes from extended Bayesian skyline plot (EBSP) analysis are reported as follows: median number of population size changes (95% HPD), and directionality of change (+ is growth; there were no instances of decline). Cases where an EBSP outcome was considered unreliable due low ESS values are indicated by ^. For each locus, the final cross-validated inference (Inf.) is given (see Methods). Reporting of multi-locus EBSP outcomes follows that of single-locus EBSPs. Species names are abbreviated as in Fig. 1

		Mitochondrial DNA						Nuclear DNA						Multi-locus
Species	BAPS cluster	F_S	R_2	*D*	*r*	EBSP	Inf.	F_S	R_2	*D*	*r*	EBSP	Inf.	EBSP
C.p.	A	−5.787*	0.038^S	−1.905*	0.139	1 (0–2) +	growth	−13.542*	0.038	−2.217*	0.265	1 (0–1) +	growth	1 (0–1)^ +
	B	0.820	0.085	−1.319	0.027	0 (0–1)	stable	0.212	0.082	−1.01	0.174	1 (0–1)^ +	stable	0 (0–1)
	C	4.972	0.131	0.561	0.011	2 (1–3) +	stable	−2.304	0.026	−1.142*	0.844	1 (0–1)^ +	stable	3 (1–4)^ +
	D	4.683	0.159	1.134	0.022	0 (0–2)	stable	−3.875	0.076	−0.672	0.098	1 (0–1)^ +	stable	0 (0–1)
	E	5.837	0.163	0.521	0.101	1 (0–3) +	stable	−3.044	0.109	−0.194	0.084	1 (0–1) +	stable	0 (0–3)^
	F	−2.479	0.075	−0.864	0.007	2 (1–3) +	stable	−21.410*	0.047	−1.085	0.044	1 (0–2)^ +	stable	2 (2–4)^ +
R.f.	A	5.353	0.133	0.467	0.114	0 (0–2)	stable	0.606	0.15	0.881	0.361	1 (0–1)^ +	stable	1 (0–3) +
	B	−5.690	0.057	−1.266	0.042	0 (0–1)^	stable	3.677	0.185^L	2.071*	0.131	0 (0–1)^	decline	0 (0–1)^
	C	10.447*	0.197^L	1.262	0.269	3 (0–3)^ +	decline	1.243	0.134	0.206	0.126	1 (0–1)^ +	stable	3 (0–3)^ +
O.d.	A (All)	−1.790	0.077	−0.395	0.150	1 (0–2) +	stable	−4.960	0.103	0.525	0.037	1 (1–1) +	stable	1 (1–1) +
S.s.	A	2.775	0.104	−0.181	0.091	3 (2–4) +	stable	−3.989	0.064	−0.997	0.063	0 (0–1)^	stable	2 (0–3)^ +
	B	1.073	0.132	−0.353	0.023	0 (0–2)	stable	−1.227	0.114	−0.473	0.018	0 (0–1)	stable	0 (0–2)
N.a.	A	0.476	0.086	−1.321	0.031	1 (0–1) +	stable	−6.940*	0.098	−0.611	0.023*	1 (1–1) +	growth	1 (0–1) +
	B	2.163	0.203	0.321	0.295	1 (0–2) +	stable	−1.333	0.135	−0.265	0.041*	1 (0–1) +	growth	0 (0–1)
	C	−1.414	0.156^S	−0.213	0.278	1 (0–3) +	growth	−0.729	0.195	−0.727	0.087	1 (0–1) +	stable	1 (0–1) +
	D	−1.390	0.262	1.168	0.313	1 (0–1) +	stable	−3.496*	0.124	−0.583	0.056	1 (1–1) +	growth	1 (0–1) +

of 9) matched corresponding single-locus inferences. The few cases of discordance included one failure of the multi-locus EBSP to detect growth in *N. americanus* cluster "B", and two apparent false positives (i.e., population size changes likely erroneously inferred for *R. flavipes* cluster "A" and *O. disjunctus*). Given our treatment of multi-locus EBSPs as confirmatory only, these did not alter our primary inferences.

Congruence Assessment

The directionality of changes in population size over time, and the geographic location where this occurred, were most concordant between *C. punctulatus* and *N. americanus* (i.e., growth/expansion in the northern region). Although neither of the two competing scenarios predicted very strong congruence between these two species, this outcome is more consistent with the ecological co-associations scenario (Fig. 2, right panel). In the southern + central region, neither of the two a priori scenarios predicted that *R. flavipes* and *N. americanus* would be outliers (i.e., decline/contraction was unique to the former, whereas growth/expansion was unique to the latter).

Historical Gene Flow Dynamics

Migration matrix estimation and hypothesis-testing using MIGRATE showed that when considering mtDNA alone, complete genetic isolation ($M = 0$) could not be rejected for all pairwise comparisons involving *C. punctulatus* clusters "C" and "D", nor for the two *S. sexspinosus* clusters (Table 3). Interestingly, analysis of mtDNA revealed that the cockroach, termite, and millipede each had a single major hub of connectivity in the central region of the study area (i.e., *C. punctulatus* cluster "E", *R. flavipes* cluster "B", and *N. americanus* cluster "B"). Furthermore, for these three species, there were no indications of any source-sink relationships (i.e., $M = s$, could not be rejected). Nuclear loci indicated much more saturated gene flow networks, with $M > 0$ inferred for all possible pairs of clusters (Table 3). For all four species that could be analyzed using MIGRATE, no single major hub was evident from nDNA. However, source-sink relationships were identified for the cockroach (3 source clusters: 1 sink), termite (1:1), and millipede (2:2), but given that there was no clear regional localization, geographic concordance could not be assessed. There was no source-sink relationship between the two centipede clusters.

Table 3. Likelihood-ratio tests (LRTs) of historical gene flow scenarios, with the null hypothesis set as either complete genetic isolation ($M = 0$), or symmetrical migration ($M = s$), for all pairwise combinations of BAPS clusters per species. Outcomes of LRTs for each single locus dataset were interpreted based on a consensus-vote across five replicate runs; if the consensus was a significant departure from the null hypothesis, the largest *P*-value is reported (number of concordant replicates given in parentheses). Not significant = "ns". Species names are abbreviated as in Fig. 1

Species	BAPS clusters	Mitochondrial DNA		Nuclear DNA	
		$M = 0$	$M = s$	$M = 0$	$M = s$
C.p.	A vs. B	ns (4)	ns (5)	<0.001 (5)	ns (5)
	A vs. C	ns (4)	ns (5)	<0.001 (4)	ns (5)
	A vs. D	ns (4)	ns (5)	<0.001 (4)	ns (5)
	A vs. E	ns (4)	ns (5)	<0.001 (4)	ns (5)
	A vs. F	ns (4)	ns (5)	<0.001 (5)	ns (5)
	B vs. C	ns (5)	ns (5)	<0.001 (5)	ns (3)
	B vs. D	ns (4)	ns (5)	<0.001 (5)	ns (3)
	B vs. E	<0.021 (3)	ns (5)	<0.001 (4)	ns (4)
	B vs. F	ns (4)	ns (5)	<0.001 (5)	<0.024 (3)
	C vs. D	ns (3)	ns (5)	<0.011 (5)	ns (5)
	C vs. E	ns (3)	ns (4)	<0.003 (4)	ns (4)
	C vs. F	ns (3)	ns (5)	<0.001 (5)	ns (5)
	D vs. E	<0.024 (4)	ns (4)	<0.001 (5)	ns (3)
	D vs. F	ns (3)	ns (5)	<0.001 (5)	<0.001 (3)
	E vs. F	<0.020 (3)	ns (5)	<0.001 (5)	<0.001 (3)
R.f.	A vs. B	<0.001 (5)	ns (3)	<0.001 (5)	ns (5)
	A vs. C	ns (5)	ns (5)	<0.001 (4)	ns (5)
	B vs. C	<0.020 (5)	ns (4)	<0.001 (5)	<0.015 (3)
S.s.	A vs. B	ns (5)	ns (5)	<0.041 (4)	ns (5)
N.a.	A vs. B	<0.018 (3)	ns (5)	<0.001 (4)	ns (4)
	A vs. C	ns (3)	ns (5)	<0.007 (5)	ns (5)
	A vs. D	ns (3)	ns (5)	<0.005 (5)	<0.002 (3)
	B vs. C	<0.025 (3)	ns (5)	<0.003 (4)	ns (5)
	B vs. D	<0.011 (5)	ns (5)	<0.001 (5)	<0.001 (5)
	C vs. D	ns (5)	ns (5)	<0.001 (5)	<0.021 (3)

Congruence Assessment

The existence, and geographic concordance, of mtDNA-based hubs of connectivity shared by *C. punctulatus*, *R. flavipes* and *N. americanus* is most consistent with predictions of the ecological co-associations scenario (Fig. 2, right panel). However, given the absence of genetic structure (and thus, any hub) in *O. disjunctus*, correspondence with this scenario's predictions was incomplete. The nDNA-based inferences also aligned most closely with the ecological co-associations scenario, given that the three species with concordant hubs were also united by the existence of source-sink gene flow relationships, to the exclusion of other species.

Discussion

Ecological Co-associations Have Power for Predicting Phylogeographic Congruence

Competing phylogeographic scenarios must be conditioned on contrasting underlying processes to be interpretable, and they also need to generate measurably different predicted outcomes to be testable (Knowles 2004). In the present paper, we focused on hypotheses in which abiotic versus biotic factors were the main drivers of responses of saproxylic invertebrates to past environmental change in the southern Appalachian Mountains. Both of these alternatives are biologically plausible: long-term habitat stability has been shown to impact how intraspecific genetic diversity is spatially distributed (e.g., Vasconcellos et al. 2019), and species interactions undoubtedly constrain or facilitate responses to Pleistocene glacial–interglacial cycles (see Introduction). For the five species studied here, expectations derived from these scenarios differed in several ways. For example, historical habitat stability predicted close congruence between the cockroach and termite, to the exclusion of the other three species (which formed a second group). Indeed, this was robust to whether occurrence records used to estimate ENMs and CS maps were cropped based on a 100 km buffer (Fig. 2, left panel) or not (Supp Fig. 4 [online only]). Conversely, the ecological co-associations scenario predicted the centipede to have the most unique phylogeographic history, and among the remaining species, *R. flavipes* and *O. disjunctus* should have been most similar, followed by *C. punctulatus* and then *N. americanus* (Fig. 2, right panel).

Given that our predictions about congruence among species were represented as a strictly bifurcating (i.e., hierarchically nested) dendrogram, yet outcomes of genetic data analyses can be equivalent among three or more species (i.e., multifurcated) or may only partly satisfy expectations, nuance becomes important when assessing fit.

Indeed, we found stronger support for the ecological co-associations scenario, but with an imperfect fit between its predictions and outcomes of empirical data analyses. Our overall conclusion that ecological co-associations have power for predicting phylogeographic congruence was based on four axes of comparison. First, geographically coinciding breaks among natural spatial-genetic clusters were identified for the cockroach, termite, and millipede (although contrary to expectations under this scenario, the beetle did not also show this same pattern). Second, the deep phylogeographic structure was shared by the cockroach, millipede, and centipede (however, the termite and beetle differed from one another, inconsistent with predictions of the ecological co-associations scenario). Third, changes in effective population size over time in the northern region of the study area were congruent between the cockroach and millipede (yet the termite and beetle were incongruent with them, and each other). Finally, historical gene flow dynamics—including hubs of connectivity and source-sink relationships—were very similar for the cockroach, termite, and millipede (but the beetle did not also show these same characteristics, which was a departure from predictions of the ecological co-associations scenario). As noted by Knowles (2009) and others, the phylogeographic parameter space is large, yet only a limited subset of scenarios can usually be examined. In our study, the two scenarios served as a useful conceptual framework, but they are highly simplified, and not mutually exclusive. Thus, conclusions about the relative importance of historical habitat stability versus ecological co-associations remain tentative.

Interestingly, if species interaction type was used as the sole component of the ecological co-associations scenario (cf., our combination of four equally weighted components), predictions would have matched outcomes much more strongly (Supp Fig. S3 [online only], bottom right). This raises the questions: what types of interactions matter most, and at what resolution do they need to be classified? For example, a distinction between facultative versus obligate antagonistic interactions may be important. On one hand, consequences of competitive exclusion can lead to allopatric distributions owing to the decreased likelihood that two or more ecologically similar species coexist (Waters 2011). Conversely, for obligate antagonistic interactions that are highly specialized (e.g., species-specific host–parasite pairs), sympatry will be maintained by host-tracking, and intrinsic dispersal and/or physiological tolerance limits of one of the interacting species can indirectly constrain responses of the other (Garrick et al. 2013). Nonetheless, there are reasons to believe that even relatively coarse classification of interaction types can be informative. For the *Sarracenia alata* pitcher plant-arthropod community, Satler et al. (2016) simply categorized species as obligate symbionts, herbivores, or capture-interrupters (i.e., those which opportunistically intercept prey that are attracted to the pitcher), yet still clearly showed that phylogeographic concordance is positively correlated with the degree of co-association. Likewise, Ortego and Knowles (2020) found that when compared to considering abiotic components of the environment alone, the addition of positive and negative interactions (i.e., facilitation and competition, respectively) between two *Quercus* oak species improved the fit of their population genomic data to intraspecific demographic models, again underscoring the potential influence of biotic drivers upon phylogeographic patterns.

Evolution of Deadwood-Dependent Invertebrates in an Unglaciated Montane Landscape

Saproxylic invertebrates typically have very limited dispersal abilities (Hammond 1984). This can be a consequence of adaptations for living in rotting logs, such as dorsoventrally flattened and/or soft bodies (Woodman et al. 2007). Also, many species are flightless despite other members of their clade having functional wings (e.g., *Panesthia* and *Cryptocercus* cockroaches), and other forms of locomotion such as jumping apparatus may have been secondarily lost (Garrick et al. 2007, 2008). In the present study, our data showed that short-range endemism was common to several focal species, and their allopatric lineages often exhibited divergences of considerable antiquity. In the southern Appalachian Mountains, similar findings have also been reported for a saproxylic opilion (Thomas and Hedin 2008). However, these same patterns also extend to arachnids associated with rocky outcrops (Keith and Hedin 2012, Hedin and McCormack 2017) and soil-burrowers (Newton et al. 2020). Indeed, the region is famous for species-level short-range endemism of plethodontid salamanders (Petranka 1998). Accordingly, regional-scale topographic complexity and steep environmental gradients are likely major divers of marked spatial-genetic structure within southern Appalachian fauna.

Interestingly, a potential "phylogeographic break hotspot" involving *C. punctulatus*, *R. flavipes* and *N. americanus* was identified between northern and central regions of the study area. Geographic sampling gaps for the latter two species precluded precise mapping of this break, but if a significant overlap is confirmed, a taxonomically broader assessment of concordance could be conducted using existing phylogeographic data from arachnids (see references above), as well as salamanders and other amphibians (e.g., Rissler and Smith 2010, Herman and Bouzat 2016, Jones and Weisrock 2018). Ultimately, the pervasiveness of a phylogeographic break across taxa with different microhabitat preferences can shed light on whether landscape-level factors were responsible, and whether the driving forces were long-standing or recurrent. Another notable finding from this study was that the central region of the study area clearly contained the largest number of distinct phylogeographic lineages aggregated across species. From a conservation perspective, parts of the central region are subject to federal environmental protection legislation, as it contains the Great Smoky Mountains National Park and adjacent lands of the Eastern Band of the Cherokee Nation, as well as several large National Forests. Thus, this region's spatial and temporal continuity of dead wood, which is critical for the long-term persistence of saproxylic invertebrate populations (Grove 2002), is probably not under immediate threat. Finally, an unexpected finding was that *O. disjunctus* showed no detectable spatial-genetic structure. We cannot rule out inadequate sampling, unexpected long-distance dispersal, or undetected recent rapid range expansion as the cause. However, this species did have distinct mtDNA clades, but they were fully sympatric—often in the same rotting logs (also see Garrick et al. 2019b, Whitaker et al. 2021). We speculate that this may be suggestive of past lineage fusion (Garrick et al. 2019c, 2020), but acknowledge that such patterns can also emerge within a single, large, unstructured population (Benham and Cheviron 2019). Additional data will be needed to test these competing ideas.

Comparative Phylogeography and the Analysis of Ecological Communities

Conceptually, comparative phylogeographic analyses can be partitioned into direct (pattern-based) and indirect (scenario-based) approaches (Garrick et al. 2008). For example, direct assessments of the extent to which co-distributed taxa have matching phylogenetic tree topologies enable inferences about co-divergence (e.g., gene tree-based tests of monophyly, Sullivan et al. 2000; species tree-based phylogeographic concordance factors, Satler and Carstens

2016). Notably, these do not rely on spatially explicit a priori hypotheses about the drivers of shared vicariance. Likewise, community trees (Carstens et al. 2016) infer the pattern of co-diversification of multiple species (after identifying and excluding outlier species), without first specifying the nature of environmental change(s) that underpin concerted responses. By contrast, the indirect means of assessing congruence rely on a common set of competing scenarios that were formulated a priori. These scenarios are based on different underlying evolutionary processes and/or events and serve as benchmarks for evaluating the fit of empirical data from each species. Such scenarios may be tailored to the landscape setting at hand, with alternative divergence and expansion/contraction events hypothesized for some areas, perhaps informed by paleoclimatic ENMs (Richards et al. 2007). Alternatively, they may be more broadly applicable. Some scenario-based approaches focus on one type of historical event (e.g., synchronous vs. asynchronous co-divergence, or co-expansion/contraction, Huang et al. 2011, Xue and Hickerson 2015). Others jointly consider a nested set of different combinations of divergence, gene flow, and population size changes (e.g., Jackson et al. 2017, Xue and Hickerson 2017). Ultimately, however, the interpretative framework is defined before results are known.

Here we attempted to incorporate elements of both direct (pattern-based) and indirect (scenario-based) assessments of congruence. We did this by first specifying a pair of competing, process-driven hypotheses (i.e., historical habitat stability vs. ecological co-associations), both of which were based on non-genetic data, thereby avoiding circularity. Fit of each species' empirical data to alternative a priori predictions were considered along four major axes of comparison. For some of these, pattern-based approaches were used (e.g., the spatial coincidence of breaks among natural spatial-genetic clusters; shared existence of phylogeographic structure). For others, we employed scenario-based approaches focusing on one type of event (e.g., the directionality of change in effective population size over time; refugial hubs of connectivity and net sources of historical gene flow). In most cases, our assessments of congruence avoided a simple dichotomy, and instead considered three or more alternative classifications. This still required considerable simplification. Indeed, the appropriate level of resolution is a difficult balance to strike between enabling broad multi-species comparisons and allowing for some inevitable idiosyncrasy (i.e., inherent "noise") versus risking failure to distinguish pseudo-congruence from true congruence.

Despite several positive aspects of our chosen analytical framework, there are also limitations. A major challenge associated with assessing the power of ecological co-associations to predict phylogeographic congruence is objectively defining the nature of species' interactions within a community. These can range from obligate to facultative, from mutualistic to antagonistic, and they may vary geographically, and throughout life cycles (Thompson 2005). Likewise, food web relationships can be dynamic across developmental stages, and fuzzy (e.g., omnivores may simultaneously occupy multiple trophic levels). Furthermore, the natural history of many species—including whether direct and/or indirect interactions occur among them—is poorly understood. Indeed, our inferences about trophic relationships were based on coarse data and relatively low sample sizes (see Garrick et al. 2019a). In the future, stable isotope analysis could be used to investigate food web structure and trophic interactions, including the nutrient flows and limitations that may shape ecological communities (Quinby et al. 2020). Brown food webs (i.e., those based on dead rather than living autotrophs) are particularly poorly understood, and these basic knowledge gaps remain to be filled. Our inferences about ecological co-associations were also partly based on patterns of succession, yet these may be variable and subject to priority effects. Regarding species interaction type and strength, there is some scope for comparative phylogeography to leverage methods developed for community ecology. For instance, Morueta-Holme et al. (2016) created a framework for inferring species associations from presence-only occurrence data (albeit limited to symmetric interactions) that corrects for indirect effects, incorporates spatial autocorrelation of species' distributions into null models, and uses network theory to identify key species in local communities that attract or repel others. Yet, despite the appeal of inferring species interactions from co-occurrence data, outcomes are prone to overinterpretation (reviewed by Blanchet et al. 2020). Indeed, our own exploratory checkerboard analyses showed sensitivity to choices about how to generate a null distribution of *C*-scores, suggesting conclusions were tenuous. In the context of terrestrial arthropods, predictive functional trait approaches (see Bartomeus et al. 2016, Brousseau et al. 2018) may provide a complementary avenue for obtaining insights into the nature of species interactions.

While comparative phylogeographic studies that characterize interaction types using very simple categories (e.g., Satler et al. 2016, Ortego and Knowles 2020) may not suffer from the same uncertainty regarding predictions of the associated "ecological co-associations scenario" as in the present study, we believe that the more finely resolved classifications attempted here will be necessary to make advances in understanding biotic influences upon present-day patterns of intraspecific genetic diversity. Indeed, several important questions remain unanswered. To what extent do ecological co-associations constrain species' responses to environmental change? At what level of co-association does the biotic constraint become negligible? What aspect(s) of species interactions matter most? To address these, study systems that include a broad gradient of co-associations, with replication at each level in the hierarchy, are particularly useful. Quantitatively characterizing interaction types, and their relative strengths, is clearly going to be very important. Although early, the findings reported here point to the potential importance of a largely overlooked component of phylogeographic history and highlight some benefits of using saproxylic invertebrates as models for disentangling the relative contributions of abiotic and biotic factors.

Supplementary Data

Supplementary data are available at *Insect Systematics and Diversity* online.

Acknowledgments

Assistance with field and/or lab work was provided by Chase Bailey, John Banusiewicz, Renan Bosque, Sabrina Bradford, Tyler Breech, Stephanie Burgess, Ethan Collier, Ben Collins, Sam Durfee, Rodney Dyer, Trey Dickinson III, Jeremy Morgan, Kayla Newton, Lee Ann Passarella, Dana Reppel, Marcella Santos, Blake Smith, Rebecca Symula, Rita Walsh, Haley Williams, and Rachel Yi. We thank Patrick Mardulyn for inviting this contribution, and Jeff Lozier and two anonymous reviewers for constructive comments on an earlier version of the paper. R.C.G. was supported by a National Science Foundation EPSCoR RII Track-4 research fellowship (award number 1738817), as well as funds from the Bay and Paul Foundations, Eppley Foundation for Research, and National Geographic Society.

Author Contributions

RCG: Conceptualization; Data curation; Formal analysis; Funding acquisition; Investigation; Methodology; Project administration; Resources; Supervision; Validation; Visualization; Writing—original draft; Writing—review & editing. CH: Data curation; Formal analysis; Investigation; Methodology; Writing—review & editing. ICA: Data curation; Formal analysis; Investigation; Methodology; Writing—review & editing. LGZ: Data curation; Formal analysis; Methodology; Writing—review & editing. PCZ: Methodology; Writing—review & editing. JCO: Formal analysis; Methodology; Writing—review & editing.

References Cited

Altschul, S. F., W. Gish, W. Miller, E. W. Myers, and D. J. Lipman. 1990. Basic local alignment search tool. J. Mol. Biol. 215:403–410.

Arbogast, B. S., and G. J. Kenagy. 2001. Comparative phylogeography as an integrative approach to historical biogeography. J. Biogeogr. 28:819–825.

Auerbach, S. I. 1951. The centipedes of the Chicago area with special reference to their ecology. Ecol. Monogr. 21:97–124.

Avise, J. C. 2000. Phylogeography: the history and formation of species. Harvard University Press, Cambridge, MA.

Bartomeus, I., D. Gravel, J. M. Tylianakis, M. A. Aizen, I. A. Dickie, and M. Bernard-Verdier. 2016. A common framework for identifying linkage rules across different types of interactions. Funct. Ecol. 30:1894–1903.

Beerli, P., and J. Felsenstein. 2001. Maximum likelihood estimation of a migration matrix and effective population sizes in *n* subpopulations by using a coalescent approach. Proc. Natl. Acad. Sci. USA. 98:4563–4568.

Benham, P. M., and Z. A. Cheviron. 2019. Divergent mitochondrial lineages arose within a large, panmictic population of the Savannah sparrow (*Passerculus sandwichensis*). Mol. Ecol. 28:1765–1783.

Blanchet, F. G., K. Cazelles, and D. Gravel. 2020. Co-occurrence is not evidence of ecological interactions. Ecol. Lett. 23:1050–1063.

Blois, J. L., P. L. Zarnetske, M. C. Fitzpatrick, and S. Finnegan. 2013. Climate change and the past, present, and future of biotic interactions. Science. 341:499–504.

Bouckaert, R., T. G. Vaughan, J. Barido-Sottani, S. Duchêne, M. Fourment, A. Gavryushkina, J. Heled, G. Jones, D. Kühnert, N. De Maio, et al. 2019. BEAST 2.5: an advanced software platform for Bayesian evolutionary analysis. PLoS Comput. Biol. 15:e1006650.

Breiman, L. 2001. Random forests. Mach. Learn. 45:5–32.

Brin, A., and C. Bouget. 2018. Biotic interactions between saproxylic insect species, pp. 471–514. *In* M. D. Ulyshen (ed.), Saproxylic insects: diversity, ecology and conservation. Springer, Heidelberg, Germany.

Brousseau, P. -M., D. Gravel, and I. T. Handa. 2018. On the development of a predictive functional trait approach for studying terrestrial arthropods. J. Anim. Ecol. 87:1209–1220.

Buisson, L., W. Thuiller, N. Casajus, S. Lek, and G. Grenouillet. 2010. Uncertainty in ensemble forecasting of species distribution. Glob. Change Biol. 16:1145–1157.

Burgess, S. M., and R. C. Garrick. 2020. Regional replication of landscape genetics analyses of the Mississippi slimy salamander, *Plethodon mississippi*. Landsc. Ecol. 35:337–351.

Carnaval, A. C., M. J. Hickerson, C. F. B. Haddad, M. T. Rodrigues, and C. Moritz. 2009. Stability predicts genetic diversity in the Brazilian Atlantic forest hotspot. Science. 323:785–789.

Carnaval, A. C., E. Waltari, M. T. Rodrigues, D. Rosauer, J. VanDerWal, R. Damasceno, I. Prates, M. Strangas, Z. Spanos, D. Rivera, et al. 2014. Prediction of phylogeographic endemism in an environmentally complex biome. Proc. R. Soc. Lond. B Biol. Sci. 281:20141461.

Carrara, F., A. Giometto, M. Seymour, A. Rinaldo, and F. Altermatt. 2015. Inferring species interactions in ecological communities: a comparison of methods at different levels of complexity. Methods Ecol. Evol. 6:895–906.

Carstens, B. C., S. J. Brunsfeld, J. R. Demboski, J. M. Good, and J. Sullivan. 2005. Investigating the evolutionary history of the Pacific Northwest mesic forest ecosystem: hypothesis testing within a comparative phylogeographic framework. Evolution. 59:1639–1652.

Carstens, B. C., M. Gruenstaeudl, and N. M. Reid. 2016. Community trees: identifying codiversification in the Páramo dipteran community. Evolution. 70:1080–1093.

Chan, Y. L., D. Schanzenbach, and M. J. Hickerson. 2014. Detecting concerted demographic response across community assemblages using hierarchical approximate Bayesian computation. Mol. Biol. Evol. 31:2501–2515.

Cheng, L., T. R. Connor, J. Siren, D. M. Aanensen, and J. Corander. 2013. Hierarchical and spatially explicit clustering of DNA sequences with BAPS software. Mol. Biol. Evol. 30:1224–1228.

Cordellier, M., and M. Pfenninger. 2009. Inferring the past to predict the future: climate modelling predictions and phylogeography for the freshwater gastropod *Radix balthica* (Pulmonata, Basommatophora). Mol. Ecol. 18:534–544.

Crespi, E. J., L. J. Rissler, and R. A. Browne. 2003. Testing Pleistocene refugia theory: phylogeographical analysis of *Desmognathus wrighti*, a high-elevation salamander in the southern Appalachians. Mol. Ecol. 12:969–984.

Cruzan, M. B., and A. R. Templeton. 2000. Paleoecology and coalescence: phylogeographic analysis of hypotheses from the fossil record. Trends Ecol. Evol. 15:491–496.

Darriba, D., G. L. Taboada, R. Doallo, and D. Posada. 2012. jModelTest 2: more models, new heuristics and parallel computing. Nat. Methods. 9:772.

Delcourt, P. A., and H. R. Delcourt. 1998. Paleoecological insights on conservation of biodiversity: a focus on species, ecosystems, and landscapes. Ecol. Appl. 8:921–934.

Di Cola, V., O. Broennimann, B. Petitpierre, F. T. Breiner, M. D'Amen, C. Randin, R. Engler, J. Pottier, D. Pio, A. Dubuis, et al. 2017. Ecospat: an R package to support spatial analyses and modeling of species niches and distributions. Ecography. 40:774–787.

Dormann, C. F., M. Bobrowski, D. M. Dehling, D. J. Harris, F. Hartig, H. Lischke, M. D. Moretti, J. Pagel, S. Pinkert, M. Schleuning, et al. 2018. Biotic interactions in species distribution modelling: 10 questions to guide interpretation and avoid false conclusions. Glob. Ecol. Biogeogr. 27:1004–1016.

Excoffier, L., and H. E. L. Lischer. 2010. Arlequin suite ver 3.5: a new series of programs to perform population genetics analyses under Linux and Windows. Mol. Ecol. Resour. 10:564–567.

Excoffier, L., and N. Ray. 2008. Surfing during population expansions promotes genetic revolutions and structuration. Trends Ecol. Evol. 123:347–351.

Excoffier, L., P. Smouse, and J. Quattro. 1992. Analysis of molecular variance inferred from metric distances among DNA haplotypes: application to human mitochondrial DNA restriction data. Genetics. 131:479–491.

Facon, B., R. A. Hufbauer, A. Tayeh, A. Loiseau, E. Lombaert, R. Vitalis, T. Guillemaud, J. G. Lundgren, and A. Estoup. 2011. Inbreeding depression is purged in the invasive insect *Harmonia axyridis*. Curr. Biol. 21:424–427.

Fu, Y. -X. 1997. Statistical tests of neutrality of mutations against population growth, hitchhiking and background selection. Genetics. 147:915–925.

Garrick, R. C. 2016. True syntopy between chromosomal races of the *Cryptocercus punctulatus* wood-roach species complex. Insectes Soc. 63:353–355.

Garrick, R. C., C. J. Sands, D. M. Rowell, N. N. Tait, P. Greenslade, and P. Sunnucks. 2004. Phylogeography recapitulates topography: very fine-scale local endemism of a saproxylic 'giant' springtail at Tallaganda in the great dividing range of south-east Australia. Mol. Ecol. 13:3329–3344.

Garrick, R. C., D. M. Rowell, C. S. Simmons, D. M. Hillis, and P. Sunnucks. 2008. Fine-scale phylogeographic congruence despite demographic incongruence in two low-mobility saproxylic springtails. Evolution. 62:1103–1118.

Garrick, R. C., P. Sunnucks, and R. J. Dyer. 2010. Nuclear gene phylogeography using PHASE: dealing with unresolved genotypes, lost alleles, and systematic bias in parameter estimation. BMC Evol. Biol. 10:118.

Garrick, R. C., J. D. Nason, J. F. Fernández-Manjarrés, and R. J. Dyer. 2013. Ecological coassociations influence species' responses to past climatic change: an example from a Sonoran Desert bark beetle. Mol. Ecol. 22:3345–3361.

Garrick, R. C., B. D. Collins, R. N. Yi, R. J. Dyer, and C. Hyseni. 2015a. Identification of eastern United States *Reticulitermes* termite species via PCR-RFLP, assessed using training and test data. Insects. 6:524–537.

Garrick, R. C., B. Kajdacsi, M. A. Russello, E. Benavides, C. Hyseni, J. P. Gibbs, W. Tapia, and A. Caccone. 2015b. Naturally rare versus newly rare: demographic inferences on two timescales inform conservation of Galápagos giant tortoises. Ecol. Evol. 5:676–694.

Garrick, R. C., Z. L. Sabree, B. C. Jahnes, and J. C. Oliver. 2017. Strong spatial-genetic congruence between a wood-feeding cockroach and its bacterial endosymbiont, across a topographically complex landscape. J. Biogeogr. 44:1500–1511.

Garrick, R. C., K. E. Newton, and R. J. Worthington. 2018. Cryptic diversity in the southern Appalachian Mountains: genetic data reveal that the red centipede, *Scolopocryptops sexspinosus*, is a species complex. J. Insect Conserv. 22:799–805.

Garrick, R. C., D. K. Reppel, J. T. Morgan, S. Burgess, C. Hyseni, R. J. Worthington, and M. D. Ulyshen. 2019a. Trophic interactions among dead-wood-dependent forest arthropods in the southern Appalachian Mountains, USA. Food Webs. 18:e00112.

Garrick, R. C., T. Dickinson III, D. K. Reppel, and R. N. Yi. 2019b. Two divergent genetic lineages within the horned passalus beetle, *Odontotaenius disjunctus* (Coleoptera: Passalidae): an emerging model for insect behavior, physiology, and microbiome research. Insects. 10:159.

Garrick, R. C., J. D. Banusiewicz, S. Burgess, C. Hyseni, and R. E. Symula. 2019c. Extending phylogeography to account for lineage fusion. J. Biogeogr. 46:268–278.

Garrick, R. C., C. Hyseni, and Í. C. Arantes. 2020. Efficient summary statistics for detecting lineage fusion from phylogeographic datasets. J. Biogeogr. 47:2129–2140.

Godsoe, W., and L. J. Harmon. 2012. How do species interactions affect species distribution models? Ecography. 35:811–820.

Gotelli, N. J. 2000. Null model analysis of species co-occurrence patterns. Ecology. 81: 2606–2621.

Graham, C. H., C. Moritz, and S. E. Williams. 2006. Habitat history improves prediction of biodiversity in rainforest fauna. Proc. Natl. Acad. Sci. U.S.A. 103:632–636.

Grove, S. J. 2002. Saproxylic insect ecology and the sustainable management of forests. Annu. Rev. Ecol. Syst. 33:1–23.

Hammond, P. M. 1984. Changes in the British coleopterous fauna, pp. 323–369. *In* D. L. Hawksworth (ed.), The changing flora and fauna of Britain. Proceedings of a Symposium of the Systematics Association, Academic Press, London, UK.

Harpending, H. C. 1994. Signature of ancient population growth in a low-resolution mitochondrial DNA mismatch distribution. Hum. Biol. 66:591–600.

Hasegawa, M., H. Kishino, and T. Yano. 1985. Dating of the human-ape splitting by a molecular clock of mitochondrial DNA. J. Mol. Evol. 22:160–174.

Hedin, M., and M. McCormack. 2017. Biogeographical evidence for common vicariance and rare dispersal in a southern Appalachian harvestman (Sabaconidae, *Sabacon cavicolens*). J. Biogeogr. 44:1665–1678.

Heled, J. 2016. Extended Bayesian skyline plot tutorial for BEAST 2. Available online: www.beast2.org/tutorials. last accessed 15 December 2020.

Heled, J., and A. J. Drummond. 2008. Bayesian inference of population size history from multiple loci. BMC Evol. Biol. 8:289.

Heller, R., L. Chikhi, and H. R. Siegismund. 2013. The confounding effect of population structure on Bayesian skyline plot inferences of demographic history. PLoS One. 8:e62992.

Herman, T. A., and J. L. Bouzat. 2016. Range-wide phylogeography of the four-toed salamander: out of Appalachia and into the glacial aftermath. J. Biogeogr. 43:666–678.

Hijmans, R. J. 2020. Raster: geographic data analysis and modeling. R package. available at https://cran.r-project.org/web/packages/raster/index.html.

Hijmans, R. J., S. E. Cameron, J. L. Parra, P. G. Jones, and A. Jarvis. 2005. Very high resolution interpolated climate surfaces for global land areas. Int. J. Climatol. 25:1965–1978.

Huang, W., N. Takebayashi, Y. Qi, and M. J. Hickerson. 2011. MTMLmsBayes: approximate Bayesian comparative phylogeographic inference from multiple taxa and multiple loci with rate heterogeneity. BMC Bioinform. 12:81.

Hugall, A., C. Moritz, A. Moussalli, and J. Stanisic. 2002. Reconciling paleodistribution models and comparative phylogeography in the Wet Tropics rainforest land snail *Gnarosophia bellendenkerensis* (Brazier 1875). Proc. Natl. Acad. Sci. USA. 99:6112–6117.

Hurvich, C. M., and C. -L. Tsai. 1989. Regression and time series model selection in small samples. Biometrika. 76:297–307.

Hyseni, C., and R. C. Garrick. 2019a. The role of glacial-interglacial climate change in shaping the genetic structure of eastern subterranean termites in the southern Appalachian Mountains, USA. Ecol. Evol. 9:4621–4636.

Hyseni, C., and R. C. Garrick. 2019b. Ecological drivers of species distributions and niche overlap for three subterranean termite species in the southern Appalachian Mountains, USA. Insects. 10:A033.

Hyseni, C., and R. C. Garrick. 2020. Data from: the role of glacial-interglacial climate change in shaping the genetic structure of eastern subterranean termites in the southern Appalachian Mountains, USA. Dryad Dataset https://doi.org/10.5061/dryad.5hr7f31

Inward, D., G. Beccaloni, and P. Eggleton. 2007. Death of an order: a comprehensive molecular phylogenetic study confirms that termites are eusocial cockroaches. Biol. Lett. 3:331–335.

Jackson, N. D., A. E. Morales, B. C. Carstens, and B. C. O'Meara. 2017. PHRAPL: phylogeographic inference using approximate likelihoods. Syst. Biol. 66:1045–1053.

Jones, K. S., and D. W. Weisrock. 2018. Genomic data reject the hypothesis of sympatric ecological speciation in a clade of *Desmognathus salamanders*. Evolution. 72:2378–2393.

Jukes, T. H., and C. R. Cantor. 1969. Evolution of protein molecules. Academic Press, New York, NY, USA.

Kearse, M., R. Moir., A. Wilson, S. Stones-Havas, M. Cheung, S. Sturrock, S. Buxton, A. Cooper, S. Markowitz, C. Duran, et al. 2012. Geneious Basic: an integrated and extendable desktop software platform for the organization and analysis of sequence data. Bioinformatics. 28:1647–1649.

Keith, R., and M. Hedin. 2012. Extreme mitochondrial population subdivision in southern Appalachian paleoendemic spiders (Araneae: Hypochilidae: *Hypochilus*), with implications for species delimitation. J. Arachnol. 40:167–181.

Knowles, L. L. 2004. The burgeoning field of statistical phylogeography. J. Evol. Biol. 17:1–10.

Knowles, L. L. 2009. Statistical phylogeography. Annu. Rev. Ecol. Evol. Syst. 40:593–612.

Lanfear, R., P. B. Frandsen, A. M. Wright, T. Senfeld, and B. Calcott. 2017. Partitionfinder 2: new methods for selecting partitioned models of evolution for molecular and morphological phylogenetic analyses. Mol. Biol. Evol. 34:772–773.

Lessa, E. P., J. A. Cook, and J. L. Patton. 2003. Genetic footprints of demographic expansion in North America, but not Amazonia, during the late Quaternary. Proc. Natl. Acad. Sci. USA. 100:10331–10334.

Loehle, C. 2007. Predicting Pleistocene climate from vegetation in North America. Clim. Past. 3:109–118.

Martin, D., and E. Rybicki. 2000. RDP: detection of recombination amongst aligned sequences. Bioinformatics. 16:562–563.

Martin, D. P., B. Murrell, M. Golden, A. Khoosal, and B. Muhire. 2015. RDP4: detection and analysis of recombination patterns in virus genomes. Virus Evol. 1:vev003.

Maynard Smith, J. 1992. Analyzing the mosaic structure of genes. J. Mol. Evol. 34:126–129.

McLachlan, J. S., J. S. Clark, and P. S. Manos. 2005. Molecular indicators of tree migration capacity under rapid climate change. Ecology. 86:2088–2098.

Messier, C., K. J. Puettmann, and K. D. Coates. 2014. Managing forests as complex adaptive systems: building resilience to the challenge of global change. The Earthscan Forest Library, Swales and Willis Ltd, Exeter, Devon, UK.

Morales-Castilla, I., M. G. Matias, D. Gravel, and M. B. Araújo. 2015. Inferring biotic interactions from proxies. Trends Ecol. Evol. 30:347–356.

Moritz, C., C. J. Hoskin, J. B. MacKenzie, B. L. Phillips, M. Tonione, N. Silva, J. VanDerWal, S. E. Williams, and C. H. Graham. 2009. Identification

and dynamics of a cryptic suture zone in tropical rainforest. Proc. R. Soc. Lond. B Biol. Sci. 276:1235–1244.

Morueta-Holme, N., B. Blonder, B. Sandel, B. J. McGill, R. K. Peet, J. E. Ott, C. Violle, B. J. Enquist, P. M. Jørgensen, and J.-C. Svenning. 2016. A network approach for inferring species associations from co-occurrence data. Ecography. 39:1139–1150.

Muscarella, R., P. J. Galante, M. Soley-Guardia, R. A. Boria, J. M. Kass, M. Uriarte, and R. P. Anderson. 2014. ENMeval: an R package for conducting spatially independent evaluations and estimating optimal model complexity for Maxent ecological niche models. Methods Ecol. Evol. 5:1198–1205.

Newton, L. G., J. Starrett, B. E. Hendrixson, S. Derkarabetian, and J. E. Bond. 2020. Integrative species delimitation reveals cryptic diversity in the southern Appalachian *Antrodiaetus unicolor* (Araneae: Antrodiaetidae) species complex. Mol. Ecol. 29:2269–2287.

Ortego, J., and L. L. Knowles. 2020. Incorporating interspecific interactions into phylogeographic models: a case study with Californian oaks. Mol. Ecol. 29:4510–4524.

Park, B., and M. J. Donoghue. 2019. Phylogeography of a widespread eastern North American shrub, *Viburnum lantanoides*. Am. J. Bot. 106:389–401.

Petranka, J. M. 1998. Salamanders of the United States and Canada. Smithsonian Institution Press, Washington, DC.

Pigot, A. L., and J. A. Tobias. 2013. Species interactions constrain geographic range expansion over evolutionary time. Ecol. Lett. 16:330–338.

Posada, D., and K. A. Crandall. 2001. Evaluation of methods for detecting recombination from DNA sequences: computer simulations. Proc. Natl. Acad. Sci. USA. 98:13757–13762.

Quinby, B. M., J. C. Creighton, and E. A. Flaherty. 2020. Stable isotope ecology in insects: a review. Ecol. Entomol. 45:1231–1246.

R Core Team. 2020. R: a language and environment for statistical computing. R Foundation for Statistical Computing, Vienna, Austria. Available at: http://www.R-project.org/.

Rambaut, A., A. J. Drummond, D. Xie, G. Baele, and M. A. Suchard. 2018. Posterior summarisation in Bayesian phylogenetics using Tracer 1.7. Syst. Biol. 67:901–904.

Ramos-Onsins, S. E., and J. Rozas. 2002. Statistical properties of new neutrality tests against population growth. Mol. Biol. Evol. 19:2092–2100.

Richards, C. L., B. C. Carstens, and L. L. Knowles. 2007. Distribution modeling and statistical phylogeography: an integrative framework for generating and testing alternate biogeographical hypotheses. J. Biogeogr. 34:1833–1845.

Riddle, B. R., and D. J. Hafner. 2006. Phylogeography in historical biogeography: investigating the biogeographic histories of populations, species, and young biotas, pp. 161–176. *In* M. C. Ebach and R. S. Tangney (eds.), Biogeography in a changing world. CRC Press, Boca Raton, FL.

Ripley, B. D. 1996. Pattern recognition and neural networks. Cambridge University Press, Cambridge, UK.

Rissler, L. J., and W. H. Smith. 2010. Mapping amphibian contact zones and phylogeographical break hotspots across the United States. Mol. Ecol. 19:5404–5416.

Rozas, J., A. Ferrer-Mata, J. C. Sánchez-DelBarrio, S. Guirao-Rico, P. Librado, S. E. Ramos-Onsins, and A. Sánchez-Gracia. 2017. DnaSP 6: DNA sequence polymorphism analysis of large data sets. Mol. Biol. Evol. 34:3299–3302.

Stone, L., and A. Roberts. 1990. The checkerboard score and species distributions. Oecologia. 85:74–79.

Salminen, M. O., J. K. Carr, D. S. Burke, and F. E. McCutchan. 1995. Identification of breakpoints in intergenotypic recombinants of HIV type 1 by bootscanning. AIDS Res. Hum. Retroviruses. 11:1423–1425.

Satler, J. D., and B. C. Carstens. 2016. Phylogeographic concordance factors quantify phylogeographic congruence among co-distributed species in the *Sarracenia alata* pitcher plant system. Evolution. 70:1105–1119.

Sawyer, S. A. 1989. Statistical tests for detecting gene conversion. Mol. Biol. Evol. 6:526–538.

Schoener, T. W. 1968. The Anolis lizards of Bimini: resource partitioning in a complex fauna. Ecology. 49:704–726.

Simberloff, D., and T. Dayan. 1991. The guild concept and the structure of ecological communities. Annu. Rev. Ecol. Syst. 22:115–143.

Smith, C. I., W. K. W. Godsoe, S. Tank, J. B. Yoder, and O. Pellmyr. 2008. Distinguishing coevolution from covicariance in an obligate pollination mutualism: asynchronous divergence in Joshua tree and its pollinators. Evolution. 62:2676–2687.

Smith, C. I., S. Tank, W. Godsoe, J. Levenick, E. Strand, T. Esque, and O. Pellmyr. 2011. Comparative phylogeography of a coevolved community: concerted population expansions in Joshua trees and four Yucca moths. PLoS One. 6:e25628.

Stamatakis, A. 2014. RAxML version 8: a tool for phylogenetic analysis and post-analysis of large phylogenies. Bioinformatics. 30:1312–1313.

Stephens, M., N. J. Smith, and P. Donnelly. 2001. A new statistical method for haplotype reconstruction from population data. Am. J. Hum. Genet. 68:978–989.

Stokland, J. N., J. Siitonen, and B. G. Jonsson. 2012. Biodiversity in dead wood: ecology, biodiversity and conservation. Cambridge University Press, Cambridge, UK.

Sullivan, J., E. Arellano, and D. S. Rogers. 2000. Comparative phylogeography of Mesoamerican highland rodents: concerted versus independent response to past climatic fluctuations. Am. Nat. 155:755–768.

Sunnucks, P., M. J. Blacket, J. M. Taylor, C. J. Sands, S. A. Ciavaglia, R. C. Garrick, N. N. Tait, D. M. Rowell, and A. Pavlova. 2006. A tale of two flatties: different responses of two terrestrial flatworms to past environmental climatic fluctuations at Tallaganda in montane southeastern Australia. Mol. Ecol. 15:4513–4531.

Swanson, A. P. 2005. Population structure in the horned passalus, *Odontotaenius disjunctus* (Illiger) (Coleoptera: Passalidae). Bachelor's Thesis, Cornell University, Ithaca, NY.

Swofford, D. L. 2003. PAUP*: phylogenetic analysis using parsimony (*and other methods). Version 4. Sinauer Associates, Sunderland, MA.

Tajima, F. 1989. Statistical method for testing the neutral mutation hypothesis by DNA polymorphism. Genetics. 123:585–595.

Tamura, K., G. Stecher, D. Peterson, A. Filipski, and S. Kumar. 2013. MEGA6: Molecular Evolutionary Genetics Analysis version 6.0. Mol. Biol. Evol. 30:2725–2729.

Tavaré, S. 1986. Some probabilistic and statistical problems in the analysis of DNA sequences. Lect. Math. Life Sci. 17:57–86.

Thomas, S. M., and M. Hedin. 2008. Multigenic phylogeographic divergence in the paleoendemic southern Appalachian opilionid *Fumontana deprehendor* Shear (Opiliones, Laniatores, Triaenonychidae). Mol. Phylogenet. Evol. 46:645–658.

Thompson, J. N. 2005. The geographic mosaic of coevolution. The University of Chicago Press, Chicago, IL.

Thuiller, W., B. Lafourcade, R. Engler, and M. B. Araújo. 2009. BIOMOD - a platform for ensemble forecasting of species distributions. Ecography. 32:369–373.

Ulyshen, M. D. 2016. Wood decomposition as influenced by invertebrates. Biol. Rev. 91:70–85.

Vasconcellos, M. M., G. R. Colli, J. N. Weber, E. M. Ortiz, M. T. Rodrigues, D. C. Cannatella. 2019. Isolation by instability: historical climate change shapes population structure and genomic divergence of treefrogs in the Neotropical Cerrado savanna. Mol. Ecol. 28:1748–1764.

Walker, M. J., A. K. Stockman, P. E. Marek, and J. E. Bond. 2009. Pleistocene glacial refugia across the Appalachian Mountains and coastal plain in the millipede genus *Narceus*: evidence from population genetic, phylogeographic, and paleoclimatic data. BMC Evol. Biol. 9:25.

Waters, J. M. 2011. Competitive exclusion: phylogeography's 'elephant in the room'? Mol. Ecol. 20:4388–4394.

Weir, B. S., and C. C. Cockerham. 1984. Estimating *F*-statistics for the analysis of population structure. Evolution. 38:1358–1370.

Whittaker, R. H. 1956. Vegetation of the Great Smoky Mountains. Ecol. Monogr. 26:1–80.

Whitaker, M., T. Procter, and F. M. Fontanella. 2021. Phylogeography and demographic expansion in the widely distributed horned passalus beetle, *Odontotaenius disjunctus* (Coleoptera: Passalidae). Mitochondrial DNA A DNA Mapp. Seq. Anal. 32:85–97.

Woodman, J. D., P. D. Cooper, and V. S. Haritos. 2007. Effects of temperature and oxygen availability on water loss and carbon dioxide release in two sympatric saproxylic invertebrates. Comp. Biochem. Physiol. A Mol. Integr. Physiol. 147:514–520.

Xue, A. T., and M. J. Hickerson. 2015. The aggregate site frequency spectrum for comparative population genomic inference. Mol. Ecol. 24: 6223–6240.

Xue, A. T., and M. J. Hickerson. 2017. MULTI-DICE: R package for comparative population genomic inference under hierarchical co-demographic models of independent single-population size changes. Mol. Ecol. Resour. 17:e212–e224.